

THE EFFECT OF METFORMIN-INDUCED AMPK ACTIVATION ON ADIPOGENESIS AND HIV REPLICATION

Kabamba Bankoledi Alexandre

A dissertation submitted to the Faculty of Health Science, University of the Witwatersrand, Johannesburg, in fulfillment of the requirements for the degree Master of Science in Medicine.

Johannesburg, 2006.

ABSTRACT

Metformin is the most common drug used against type 2 diabetes mellitus. However, it was only recently shown, in human and rat hepatocytes, that metformin-like 5-aminoimidazole-4-carboximide ribonucleoside (AICAR), acts via activation of the AMP-activated protein kinase (AMPK), an enzyme that plays a central role in lipid metabolism. Although it is well known that metformin is used in the treatment of type 2 diabetes and results in significant fat loss, no study has investigated the effects of this drug on adipocytes. In this report I studied the effects of metformin on the formation of fat deposits in mouse 3T3-L1 pre-adipocytes, as well as its effects on the activation of AMPK in these cells. Our results suggested that metformin significantly inhibits the transformation of pre-adipocytes into adipocytes. This is achieved via the inhibition of intracellular lipid accumulation during adipogenesis. In addition to its inhibition of intracellular lipid accumulation, metformin induced a significant increase in the phosphorylation of AMPK. It has been shown that AMPK activation with AICAR results in the inhibition of the nuclear factor- κ B (NF- κ B) induced gene expression. Since NF- κ B is the key nuclear factor used by HIV-1 during the initiation of its gene transcription, I investigated the possibility of inhibiting HIV-1 replication in U1 cells with metformin and AICAR. I observed that AICAR and metformin inhibit HIV-1 replication in U1 cells. This inhibition was

paralleled by the accumulation of NF- κ B in the cytoplasm of AICAR and metformin treated cells, and at the same time by a significant decrease in the concentration of this nuclear factor in the nucleus of these cells.

However, I failed to observe any phosphorylation of AMPK by metformin and AICAR in U1 cells.

In conclusion, metformin inhibits adipogenesis in mouse adipocytes and this inhibition is likely to take place via the activation of AMPK. AICAR and metformin have inhibitory properties against HIV-1 replication. However, this inhibition does not seem to be by the activation of AMPK.

DECLARATION

I declare that this dissertation is my own work and that it has not been submitted for any other degree or examination in any other University.

Since this study was performed using cell lines, we did not require ethical clearance from the University of the Witwatersrand Committees for Research on Humans or Animal Subjects.

Kabamba Bankoledi Alexandre

.....day of.....2006.

ACKNOWLEDGEMENTS

I would like to thank the South African Medical Research Council (MRC), the National Research Foundation (NRF), the National Health Laboratory Services (NHLS) Research Trust, and the Richard Ward Endowment Trust, University of the Witwatersrand, for funding this research.

Many thanks to Professor Lynn Morris and Elin Gray, from the National Institute of Communicable Diseases, for their contribution to this study. Also thanks to all the staff members of the Department of Chemical Pathology, Faculty of Health Science, University of the Witwatersrand for their direct and indirect contributions to this work. Finally, thanks to my supervisors Professor Nigel John Crowther and Ms Aletta Maria Smit for everything they have done for this study to be a success.

PRESENTATIONS

1. We presented the paper: Elucidating the mechanism of metformin action in fat cells, by Alexandre, K.B., A.M. Smit, and N.J. Crowther; at the University of the Witwatersrand, Faculty of Health Science Research Day 2004. The presentation was awarded the prize for best oral presentation in the Basic Health Science and Chronic Disease category.
2. We presented the paper: Metformin inhibits intracellular lipid accumulation in the murine preadipocyte cell line, 3T3-L1, by Alexandre, K.B., A.M. Smit, and N.J. Crowther; at the 41st meeting of the Society for Endocrinology, Metabolism and Diabetes of South Africa (SEDMSA), in April 2005.

3. We presented the poster: AICAR and metformin inhibit HIV-1 replication in U1 cells; by Alexandre K.B., E. Gray, A. Smit, L. Morris, and N. Crowther, at the University of the Witwatersrand Research Day 2006. The poster was awarded the prize for best poster presentation in HIV and Infectious Diseases category.

4. We presented the poster: metformin inhibits intracellular lipid accumulation in the murine preadypocyte cell line 3T3-L1; by Alexandre K.B., A.M. Smit, P. Gray and N.J. Crowther, at the Cell Signalling Symposium in 2005 at Dundee, U.K.

TABLE OF CONTENTS

Chapter 1: Literature Review	1
1.1 Introduction.....	2
1.2 AMPK structure.....	5
1.2.1 AMPK isoforms.....	5
1.2.2 AMPK Isoform expression and their role in adaptation to intense physical training.....	8
1.3 AMPK activators.....	10
1.3.1 Metformin.....	10
1.3.1.1 Biochemistry of metformin.....	10
1.3.1.2 Metformin side effects.....	13
1.3.2 AICAR.....	14
1.3.2.1 Biochemistry of AICAR.....	14
1.4 AMP-activated protein kinase.....	16
1.4.1 LKB1.....	16
1.4.2 Ca ⁺⁺ /calmodulin-dependent protein kinase kinase (CAMKK).....	17
1.5 Cellular effects of AMPK.....	18
1.5.1 AMPK mediates glucose transport in muscle.....	18
1.5.2 AMPK involvement in the nitric oxide signaling system.....	19
1.5.3 Role of AMPK in the regulation of the sympathetic nervous system.....	20
1.5.4 AMPK may regulate gene expression.....	21
1.5.5 AMPK inhibition of intracellular lipid accumulation.....	22
1.6 AMPK and type 2 diabetes mellitus.....	24
1.6.1 Obesity and insulin resistance.....	25

1.6.2 The possible role of AMPK in the aetiology of type 2 diabetes.....	26
1.7 AMPK and HIV-1 replication.....	28
1.7.1 HIV-1 classification.....	29
1.7.2 HIV-1 structure and life cycle.....	31
1.7.3 HIV-1 infectivity.....	35
1.7.4 HIV-1 genome.....	37
1.7.5 Nuclear factor- B and HIV-1 replication.....	37
1.7.6 NF- B cooperates with the viral protein Tat to initiate HIV-1 replication.	41
1.7.7 NF- B cis-acting motifs regulate HIV-1 transcription in human macrophages.....	42
1.7.8 TNF- initiate HIV-1 replication via NF- B.....	44
1.7.9 AMPK inhibition of transcriptional activators used by HIV-1.....	44
1.7.10 HIV treatment.....	45
1.8 Aims of the study.....	46
Chapter 2: Materials and Methods.....	47
2.1 AMPK inhibition of adipogenesis.....	48
2.1.1 Optimization of AICAR and metformin concentration for adipogenesis	48
2.1.2 3T3-L1 cell culture, treatment with AICAR and metformin, and initiation of adipogenesis.....	50
2.1.3 Detection of AMPK phosphorylation by AICAR and metformin.....	50
2.1.4 3T3-L1 trypsinization.....	51
2.1.5 Oil red O preparation.....	52
2.1.6 Oil red O staining.....	52

2.1.7 Protein extraction from 3T3-L1	53
2.1.8 Determination of protein concentration using the Bradford method.....	54
2.2 AICAR and metformin inhibition of HIV-1 replication in U1 cells.....	55
2.2.1 Optimization of AICAR and metformin concentration for HIV-1 inhibition in U1 cells.....	55
2.2.2 U1 cell culture and treatment with AICAR and metformin.....	57
2.2.3 HIV-1 p24 antigen ELISA.....	58
2.2.4 U1 cells protein extraction.....	60
2.3 Western Blotting.....	61
2.3.1 Protein electrophoresis.....	61
2.3.2 Protein transfer to the Immobulon-P membrane.....	62
2.3.3 Drying the membrane after protein transfer.....	63
2.3.4 Rapid chemiluminescent detection of proteins on the Immobulon-P membrane.....	64
2.3.5 Amido black staining.....	66
2.3.6 Statistical analysis.....	67
Chapter 3: Results.....	68
3.1 3T3-L1 results.....	69
3.1.1 Optimization of AICAR and metformin concentration for adipogenesis...	69
3.1.2 Comparing 3T3-L1 lipid content at confluence (day 0) and at the end of adipogenesis (day 8) and after treatment with AICAR and metformin.....	70
3.1.3 Comparing protein concentration of 3T3-L1 treated with metformin or AICAR and the control cells.....	72
3.1.4 Western blotting of phosphor-AMPK.....	73

3.2 U1 results.....	76
3.2.1 Optimization of AICAR and metformin concentration for inhibition of HIV-1 replication in U1 cells.....	76
3.2.2 NaCl activates HIV-1 replication in U1 cells.....	79
3.2.3 AICAR and metformin inhibit HIV-1 replication in U1 cells.....	81
3.2.4 AICAR and metformin inhibit NF- B translocation from the cytoplasm to the nucleus.....	85
3.2.5 AMPK expression in U1 cells.....	91
3.2.6 AICAR and metformin do not phosphorylate AMPK at threonine 172 in U1 cells.....	93
Chapter 4: Discussion.....	95
4.1 Metformin inhibits adipogenesis in 3T3-L1.....	96
4.2 Metformin and AICAR inhibit HIV-1 replication in U1 cells.....	100
Appendix.....	105
Appendix I reagents.....	106
Appendix II: buffers and solutions for protein electrophoresis and Western blotting.....	108
Appendix III: raw data.....	117
List of References.....	130

List of illustrations

Figure 1.1: AMPK pathways.....	4
Figure 1.2: AMPK isoforms and their components.....	7
Figure 1.3: Chemical structure of metformin.....	10
Figure 1.4: Diagram depicting HIV-1 structure.....	31
Figure 1.5: HIV-1 capsid structure.....	32
Figure 1.6: Interaction of HIV-1 gp120 and gp41 with CD4 and CCR5....	34
Figure 1.7: Diagrammatic representation of HIV-1 life cycle.....	35
Figure 1.8: A photograph of HIV budding from a T-cell.....	36
Figure 1.9: Chemical structure of the most abundant member of the NF- B family.....	39
Figure 1.10: Pathway of I B degradation and release of NF- B.....	40
Figure 3.1: Graph of metformin and AICAR inhibition of adipogenesis in 3T3-L1	70
Figure 3.2: Western blotting of metformin treated, AICAR treated, and untreated 3T3-L1 on day 0 and after 8 days of adipogenesis.....	74
Figure 3.3: Graph comparing the level of AMPK phosphorylation in 3T3-L1 on day 8 for metformin and AICAR treated cells against the negative control.....	75
Figure 3.4: Graph of U1 cells count against AICAR and metformin concentrations.....	77

Figure 3.5: Graph of the optimization of AICAR and metformin concentration for use against HIV-1 in U1 cells.....78

Figure 3.6: Graph of HIV-1 activation in U1 cells with 60 mM NaCl..... 80

Figure 3.7: Graph of p24 concentration after the inhibition of HIV-1 replication by AICAR and metformin.....82

Figure 3.8: Photograph of the Western blotting of the cytoplasmic and nuclear extract of U1 cells with anti-NF- B antibody..... 86

Figure 3.9: Graph comparing the concentration of the cytoplasmic and nuclear NF- B of AICAR and metformin treated U1 cells compared to control cells..... 88

Figure 3.10: Photograph of the amido black stained membrane used for Western blotting of the cytoplasmic extracts of U1 cells..... 89

Figure 3.11: Photograph of the amido black stained membrane used for the Western blotting of the nuclear extracts of U1 cells.....90

Figure 3.12: Photograph of the Western blotting of the γ -subunit of AMPK in U1 cells cytoplasm.....92

Figure 3.13: Western blotting of phospho-AMPK in 3T3-L1 compared to the Western blotting of phospho-AMPK in U1 cells.....94

List of tables

Table 3.1: Comparing the protein concentrations of 3T3-L1 treated with metformin or AICAR and the control cells.....72

Table 3.2: Mean p24 values as percentage of controls, after 2 days of tissue culture, for U1 cells treated with metformin.....83

Table 3.3: Mean p24 values as percentage of controls, after 2 days of tissue culture, for U1 cells treated with AICAR.....84

List of abbreviations

AMPK:	AMP-activated protein kinase
AMPKK:	AMP-activated protein kinase kinase
ATP :	Adenosine triphosphate
AMP :	Adenosine monophosphate
HNF4 :	Hepatocyte-specific nuclear factor 4
NF- B :	Nuclear factor kappa B
AICAR:	5-aminoimidazole-4-carboximide ribonucleoside
HUVEC:	Human umbilical vein endothelial cells
eNOS :	Endothelial nitrous oxide synthase
T2DM:	Type 2 diabetes
CBS :	Cystathionine -synthase
KIS :	Kinase interacting sequence
ASC :	Association with SNF1 sequence
ZMP :	AICA ribotide
GLUT4:	Glucose transporter 4
GLUT2:	Glucose transporter 2
PEPCK:	Phospho-enolpyruvate carboxykinase
G6Pase:	Glucose-6-phosphatase
SnF1 :	Sucrose non-fermenting1
IGF1 :	Growth factor-1

ATM :	Ataxia telangiectasia
STRAD /STRAD :	Ste20-related adaptor protein- or -
MO25 /MO25 :	Mouse protein-25 or -
CAMKK:	Ca ⁺⁺ /calcium-dependent protein kinase kinase
siRNA:	Small interfering RNA
NO :	Nitric oxide synthase
nNOS :	Neural nitric oxide synthase
L-PK :	Liver type pyruvate kinase
FAS :	Fatty acid synthase
PGC1 :	Peroxisome proliferators-activated receptor coactivator 1
NRF1 :	Nuclear respiratory factor 1
MF2 :	Mesoderm/mesenchyme forkhead 2
HUR :	Human -antigen R
C/EBP :	CCAAT/enhancer-binding protein
PPAR :	Peroxisome proliferator activated receptor
aFABP/aP2:	Adipocyte fatty acid binding protein
cAMP :	Cyclic AMP.
HSL :	Hormone sensitive lipase
PKA :	Protein kinase A
TNF :	Tumor necrosis factor
FFA :	Free fatty acid
ACC- :	Acetyl-CoA carboxylase

SIV	:	Simian immunodeficiency virus
LTR	:	Long terminal repeat
RHD	:	Rel homology domain
I- B	:	Inhibitor kappa B
IKK	:	I B kinase
MSK-1:		Mitogen- and stress-activated protein kinase-1
PMA	:	Phorbol myristate acetate
PHA	:	Phytohemagglutinin
NRTI	:	Nucleoside analogue reverse transcriptase inhibitor
NNRTI:		Non-nucleoside analogue reverse transcriptase inhibitor
PI	:	Protease inhibitor
HAART:		Highly active anti-retroviral therapy
IBMX	:	3-isobutyl-1-methylxantine
PBS	:	Phosphate buffered saline
HRP	:	Horse radish peroxidase
OD	:	optical density
TBS-T	:	Tris-buffered saline
ECL	:	Enhanced chemiluminescent
SREBP-1:		Sterol regulatory enhancer binding protein
DMEM:		Dulbecco modified Eagle's medium
FCS	:	Foetal calf serum
Thr-172:		Threonine 172

CHAPTER 1
LITERATURE REVIEW

1.1 Introduction

Adenosine monophosphate-activated protein kinase (AMPK) is a major regulator of cellular energy metabolism. AMPK is activated under conditions such as exercise and starvation, that decrease the intracellular concentration of adenosine triphosphate (ATP) and increase the concentration of adenosine monophosphate (AMP) [1]. The ratio (ATP)/ (AMP) regulates the activation of AMPK i.e. a decrease in the ratio activates AMPK while an increase inactivates the enzyme. In addition to regulating intracellular energy homeostasis, AMPK modulates whole body energy expenditure by controlling processes such as food intake. It has been shown that in the region of the rat hypothalamus that controls food intake and satiety, AMPK inhibition by leptin and insulin inhibits food intake, while its activation by the gut hormone ghrelin stimulates this process [2].

AMP regulates AMPK activation via allosteric control. The binding of AMP to AMPK induces a change in conformation that makes AMPK susceptible to phosphorylation at residue threonine-172 (Thr-172) of its catalytic subunit, or α -subunit, by an upstream kinase known as AMPK kinase (AMPKK) [1, 3, 4]. LKB1 has been identified as one of the upstream kinases that phosphorylate AMPK [1, 5]. The activated AMPK phosphorylates and inhibits key enzymes involved in pathways that

consume ATP, such as fatty acid and cholesterol biosynthesis, and at the same time it activates pathways that produce ATP, such as the β -oxidation of fatty acids and glycolysis (figure 1.1).

Gene transcription is also inhibited by AMPK under conditions of low ATP concentration, as this process requires energy [6]. AMPK inhibition of gene expression is via inhibition of transcription factors such as Nuclear factor- κ B (NF- κ B) and hepatocyte-specific nuclear factor 4 α (HNF4 α) [1, 6]. It has been shown that NF- κ B induced gene expression can be suppressed by AMPK activation with 5-aminoimidazole-4-carboximide ribonucleoside (AICAR), in human umbilical vein endothelial cells (HUVEC) [1]. This opens up the possibility of using the activation of AMPK against viruses such as the human immunodeficiency virus type 1 (HIV-1) which depend on NF- κ B to induce their gene transcription [7].

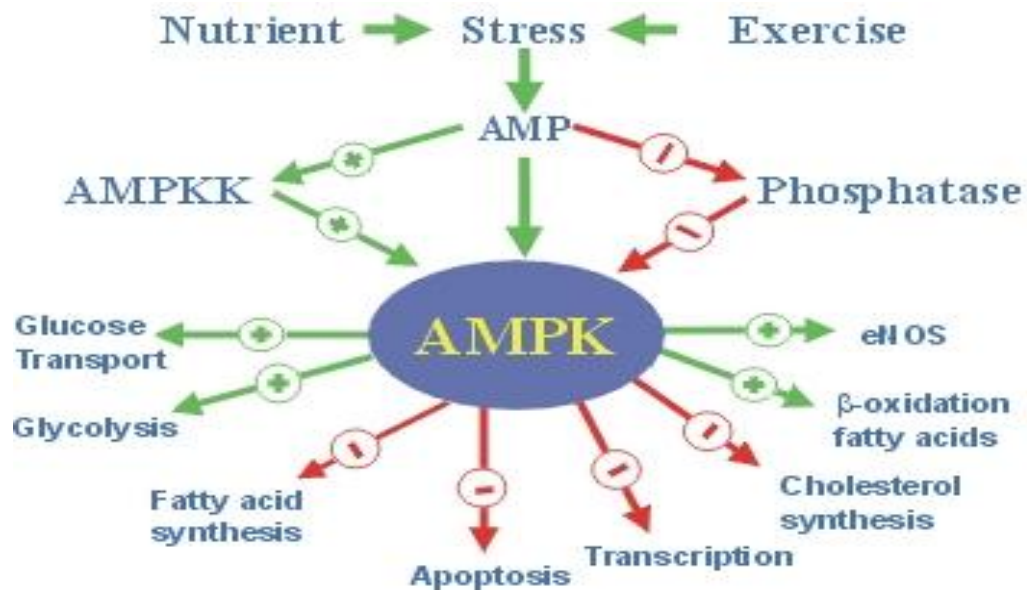


Figure 1.1: Pathways inhibited by AMPK activation are shown in red. Pathways that activate AMPK and those that are activated by AMPK activation are shown in green [1] (eNOS: endothelial nitrous oxide synthase).

Deficiencies in the AMPK signaling system have been implicated in many metabolic disorders, amongst them type 2 diabetes (T2DM) and obesity [8].

Metformin is a drug that is widely used against T2DM and insulin resistance, and it is believed to act via activation of AMPK [9].

1.2 AMPK structure

1.2.1 AMPK-isoforms

AMPK is an α -heterotrimer. The α -subunit is the catalytic subunit, whilst the β - and γ -subunits are non-catalytic, but they are required for the stability of the heterotrimer and for substrate specificity. There are two β -subunits, β_1 and β_2 , two γ -subunits, γ_1 and γ_2 , and three α -subunits, α_1 , α_2 , and α_3 . All possible combinations of these AMPK subunit isoforms give active complexes. AMPK is activated by phosphorylation at the threonine-172 residue of the α -subunit. The binding of AMP to AMPK γ -subunit results in the allosteric activation of AMPK. This binding also makes AMPK susceptible to phosphorylation at the catalytic subunit by upstream kinases. Lastly, AMP binding inhibits AMPK dephosphorylation by protein phosphatases. AMPK activation by phosphorylation results in a 50 - 100 fold increase in AMPK activity, compared to a 5-fold increase during allosteric activation [2].

AMPK γ -subunits have tandem pairs of the cystathionine β -synthase (CBS) domain (named after the enzyme cystathionine β -synthase) (figure 1.2) [2, 10]. Each pair binds to either one AMP or ATP molecule. The first cystathionine β -synthase pair (cystathionine β -synthase 1 and 2) creates a binding site for AMP around arginine-70, histidine-151, arginine-152 and arginine-171. Mutations in Arg-70, Arg-152, and Arg-171 results in the loss of AMP dependence, resulting in a constitutively

active enzyme. It has been proposed [10] that ATP binding to the CBS domain allows ATP to bridge the α -subunit activation site and interacts with molecules that interact with the phospho-threonine-172. This leads to the unavailability of threonine-172 for phosphorylation. Contrary to ATP, when AMP binds to this site the bridging of the α - and γ -subunits does not occur and threonine-172 becomes available for phosphorylation. When threonine-172 is phosphorylated the bridging of the α - and γ -subunits exposes the residue to phosphatases for dephosphorylation, while AMP binding to CBS shields threonine-172 from phosphatases [10].

The AMPK β -subunit contains two domains named kinase interacting sequence (KIS) and association with SNF1 sequence (ASC). The ASC domain is involved in the formation of β -complex, while the KIS domain is thought to play a role in the binding of glycogen [2].

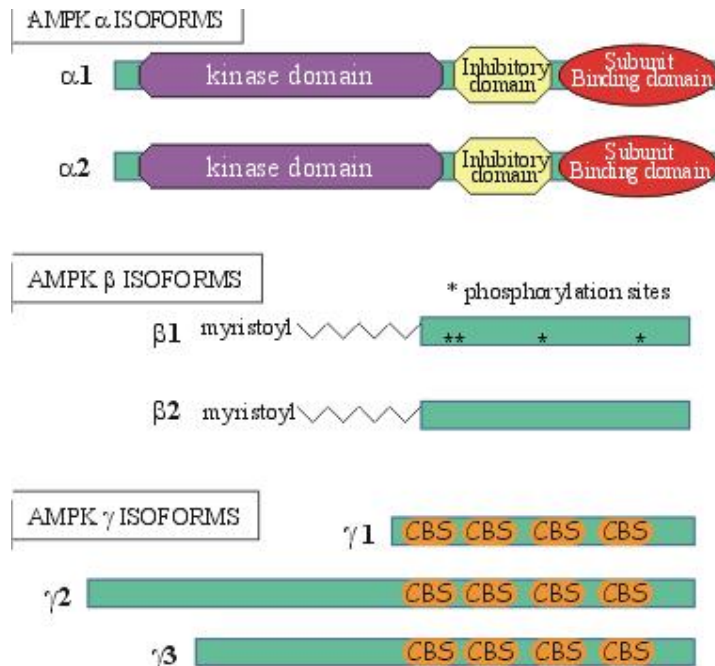


Figure 1.2: AMPK isoforms and their components: the catalytic site, the inhibitory domain, and the subunit binding domain of α isoforms; the phosphorylation sites of β isoforms; the CBS domains of γ -isoforms [1].

1.2.2 AMPK isoform expression and their role in adaptation to intense physical training

Winder and colleagues [11] suggested that the expression of different AMPK-subunits is tissue specific. In their study conducted in rats, the α_1 -subunit was found to be mainly expressed in slow twitch soleus and fast twitch red vastus lateralis muscle, whilst the α_2 -AMPK subunit was the main subunit in the fast twitch red and white vastus lateralis muscles, while its expression was low in the slow twitch soleus muscle. The α_1 -subunit was highly expressed in the slow twitch soleus muscle, while the α_2 -subunit was mainly present in the fast twitch red and white vastus lateralis muscles. The α_1 -subunit was abundant in the fast twitch white vastus lateralis muscle and the α_3 -subunit was mainly expressed in the fast twitch white vastus lateralis and slow twitch soleus muscles.

Similarly, it was shown that α_2 is mainly expressed in rat fast twitch red vastus lateralis muscle.

It is also important to note that the AMPK α_1 -subunit is widely distributed in different body tissues while the α_2 -subunit is primarily expressed in skeletal muscle, heart and liver. It has been suggested that the difference in the expression pattern of AMPK in different tissues is related to the energy need of the tissue concerned. For example, the slow twitch soleus fibers, where the α_1 is highly expressed, have a

higher capacity for synthesizing ATP, and they contain many mitochondria and are utilized for endurance activities.

It is also possible that the adaptation of professional athletes to intense physical training is mediated by AMPK. Durante *et al.* [12] observed that endurance trained rats had a reduced activation of AMPK during an acute bout of exercise compared to their untrained counterparts.

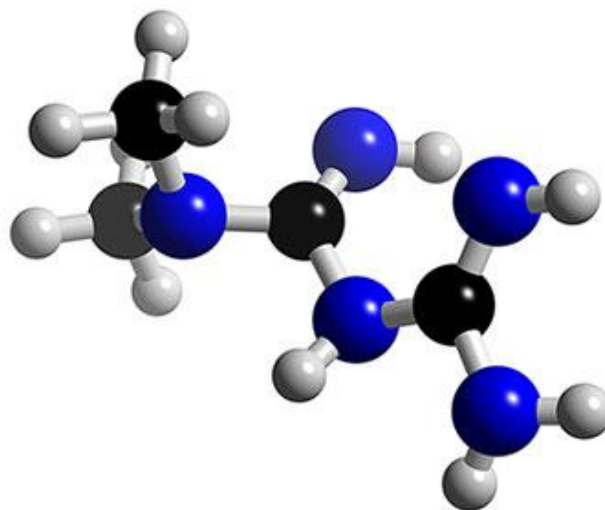
Durante and colleagues [12] explained this attenuation of AMPK by a change in gene expression that results in a moderate degree of metabolic stress, this in turn leading to a more modest effect on AMP, ATP, and phosphocreatine levels. Note that in the cell ATP is directly generated from phosphocreatine [13]. The red quadriceps muscles of trained rats have a higher content of glycogen compared to untrained rats. Elevated glycogen content in muscle has been reported to greatly attenuate AMPK activation by muscle contraction. These findings are supported by a similar observation in humans where AMPK in skeletal muscle of trained individuals is found to be less activated during intense physical activities, in comparison to untrained individuals [14].

1.3 AMPK activators

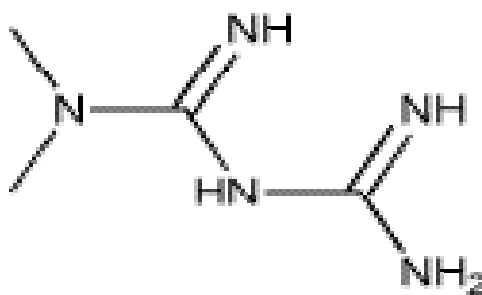
1.3.1 Metformin

1.3.1.1 Biochemistry of metformin

A.



B.



Chemical Formula: $C_4H_{11}N_5$

Figure 1.3: 3 dimensional structure of metformin (A). Chemical structure of 1,1-dimethyl biguanide or metformin (B) [15].

Metformin (figure 1.3 (A) and (B)) is one of the most commonly used drugs for the treatment of type 2 diabetes. Although metformin has been in use since 1957 its exact mechanism of action remained unclear until recently [16]. Metformin is believed to reduce type 2 diabetes related mortality and the susceptibility to myocardial infarction and stroke, via its effects on lipid metabolism [17]. In addition to its well documented ability to increase glucose uptake in skeletal muscles and adipocytes, metformin also inhibits hepatic glucose output. Cleasby and colleagues [17] proposed that metformin normalizes hepatic glucose output by acting on key gluconeogenic enzymes, such as pyruvate carboxylase, pyruvate kinase, and glucose-6-phosphatase. This increases liver glycogen production while decreasing glucose production.

One study has shown that similar to diet and exercise, metformin reduces the risks of developing type 2 diabetes in insulin resistant individuals [18]. Progression to type 2 diabetes is also prevented in obese individuals by the use of metformin [17].

Recently, there have been many studies that suggested that metformin acts by activating AMP-activated protein kinase [9, 19]. Musi and colleagues [18] showed that metformin treatment for 10 weeks significantly increased AMPK- α_2 activity in skeletal muscle of type 2 diabetic individuals. Although this study suggested that metformin can

change the cell energy status via alteration of the AMP/ATP ratio, metformin activation of AMPK is widely believed to be via activation of the kinase, LKB1 [20]. Nevertheless, Hawley and colleagues [21] suggested that the effects of metformin on AMPK is not mediated by any of the known AMPK kinases. Hawley and colleagues also proposed that metformin may be a pro-drug that is transformed intracellularly to its active form. Since metformin is mostly excreted in urine in an unaltered form, these investigators believe this hypothetical active species may represent only a minor fraction of the administered drug. Another interesting suggestion of the mechanism of metformin activation of AMPK came from Owen *et al.* [21]. This group suggested that metformin inhibition of complex I of the electron transport chain results in the lowering of the intracellular energy charge, ultimately resulting in AMPK activation. This hypothesis, however, was refuted by Hawley *et al.* who showed that metformin could activate AMPK even in cells that did not use the respiratory chain to produce ATP [21].

1.3.1.2 Metformin side effects

The most common side effects of metformin are weight loss and lactic acidosis [16, 22, 23]. The latter occurs mainly in patients with contraindications to the drug, such as alcoholism, renal impairment, severe cardiorespiratory disease, liver dysfunction and hemodynamic instability. It has been suggested that lactic acidosis caused by metformin is due to its inhibition of gluconeogenesis from alanine, pyruvate, and lactate, resulting in an excessive increase in plasma lactate concentration [18, 22]. However, Owen *et al.* proposed that the main cause of metformin induced lactic acidosis is the inhibition of complex I of the electron transport chain which results in pyruvate being converted solely to lactate, instead of also entering the citric acid cycle [18, 21].

Weight loss associated with metformin is widely believed to be due to metformin's action on key enzymes of lipid metabolism [23].

Interestingly, it has been observed that metformin can also induce weight loss by decreasing net caloric intake, most probably via the suppression of appetite [16].

Other side effects of metformin, although of lesser importance, include diarrhoea, flatulence, and abdominal discomfort. Long term use of metformin can also lead to vitamin B₁₂ malabsorption, resulting in a

decrease of vitamin B₁₂ intracellular concentrations and bioavailability [16].

1.3.2 AICAR

1.3.2.1 Biochemistry of AICAR

AICAR is a nucleoside analog that enters the cell, through nucleoside transporters, where it is phosphorylated and converted to the nucleotide AICA ribotide (ZMP) by adenosine kinase. In the cell ZMP mimics the effects of AMP. Like metformin, AICAR stimulates glucose uptake in skeletal muscle by inducing the translocation of GLUT4 to the cytoplasmic membrane of muscle cells. The administration of AICAR in rats has been reported to induce a 30-40% decrease in adipose tissue mass [24]. However, though, widely used as an activator of AMPK, AICAR is not specific in its metabolic activities. AICAR also activates other AMP-regulated enzymes such as glycogen phosphorylase of the glycogenolysis pathway and fructose-1, 6-bisphosphate of the gluconeogenic pathway [21, 25]. A major advantage of using AICAR, in the study of the AMPK signaling system, is that it does not alter the intracellular levels of ATP, ADP, and AMP, thus any changes observed in AMPK activity cannot be due to the alteration of the intracellular (ATP)/(ADP)(AMP) ratios [26] but due to an increase in ZMP concentration. A study by Lochhead and colleagues [26] showed that

AICAR in rat hepatoma cells (4HIIIE) mimics insulin by suppressing the gene expression of phospho-enolpyruvate carboxykinase (PEPCK) and glucose-6-phosphatase (G6Pase). Gene products of PEPCK and G6Pase are key regulators of gluconeogenesis in the liver. Defects in the regulation of PEPCK and G6Pase gene products have been associated with type 2 diabetes. PEPCK and G6Pase are found to be over expressed in tissues that have lost sensitivity to insulin [26]. Lochhead and colleagues believe that the effect of AICAR on PEPCK and G6Pase gene expression is through AMPK. This is consistent with the report that AMPK can also regulate cell energy metabolism at the level of gene expression [6]. This is supported by the report that constitutive activation of AMPK inhibits PEPCK gene expression [27].

AICAR is used pharmacologically, under the name acadesine, to treat ischemic heart disease. During ischemic stress acadesine acts as a free radical-scavenger, reacting with oxidants released by neutrophils. Acadesine is also reported to act via inhibition of adenosine deaminase, thus, increasing the concentration of adenosine. Adenosine plays a major role in the protection of body tissues during ischemia [28, 29].

1.4 AMP-activated protein kinase kinase.

1.4.1 LKB1

The yeast AMPK homologue, sucrose non-fermenting1 (Snf1), like AMPK, is activated by phosphorylation at a threonine residue of its catalytic subunit, the Snf1 p-subunit. As shown by Hong and colleagues [30] in both *in vitro* and *in vivo* studies, Snf1 is phosphorylated by upstream kinases Pak1p, Tos3p, and Elm1p. Hong's research group also found that Tos3p was able to phosphorylate mammalian AMPK. Tos3p is the yeast equivalent to mammalian LKB1. This enzyme is a 50 kDa serine/threonine protein kinase. The product of the LKB1 gene is mutated in the Peutz-Jeghers syndrome which is characterized by an increase in the risk of developing multiple tumors in various tissues [31]. Shaw *et al.* [5] demonstrated that LKB1-deficient murine embryonic fibroblasts have an almost complete loss of both threonine-172 phosphorylation of AMPK and downstream signaling in response to AMPK activators. Investigators have also been able to show that AMPK activation by metformin and exercise, is achieved via LKB1 [20].

However, a study by Suzuki *et al.* [32] suggested that there may also be a LKB1-independent pathway in the AMPK signaling system. Suzuki *et al.* observed that the phosphorylation of AMPK could also be induced by insulin like growth factor-1 (IGF-1). Suzuki and co-workers proposed that the induction of AMPK activation by this growth factor is achieved

via the ataxia telangiectasia mutated molecule (ATM), as any inhibition of this kinase expression resulted in the abolition of AMPK activation by IGF-1. ATM is involved in the p53 signaling system [32]. It is interesting to note that AMPK phosphorylation by IGF-1 could be induced even in LKB1-nonexpressing HeLa cells [32]. Lizcano and colleagues [33] also observed that phenformin, a drug closely related to metformin, activates AMPK via an LKB-1 independent mechanism.

Hawley *et al.* [31] reported that LKB1 acts in association with other proteins to achieve its kinase activity. This research group showed that AMP-Kinase kinase (AMPKK) is a complex of proteins made up of LKB1, Ste20-related adaptor protein- α or - β (STRAD α /STRAD β) and mouse protein-25 α or - β (MO25 α /MO25 β). The ability of this complex to activate AMPK was dependent on LKB1 activity as an AMPKK. The complex LKB1:STRAD:MO25 has also been shown to phosphorylate and activate at least 12 other kinases of the AMPK subfamily [33].

1.4.2 Ca⁺⁺/Calmodulin-dependent protein kinase kinase

Members of the Ca⁺⁺/calmodulin-dependent protein kinase kinase (CAMKK) family, CAMKK α and CAMKK β , show significant sequence homology with LKB1, Elm1p, Tos3p and Pak1p [34]. Hurley *et al.* [34] studying the AMPK signaling system in 3 cell lines deficient in LKB1 found that mannitol, 2-deoxyglucose and ionomycin activate AMPK by

phosphorylation. This phosphorylation and that of enzymes downstream were inhibited by the CAMKK inhibitor, STO-609 and CAMKK siRNAs. CAMKK α is activated by Ca⁺⁺, while CAMKK β is constitutively activated, although its activity is also stimulated by a rise in the Ca⁺⁺ concentration.

Leclerc and Rutter [6] showed that an increase in Ca⁺⁺ concentration due to cell depolarization by KCl activates AMPK via CAMKK. Leclerc and Rutter also suggested that metabolisable amino acids such as leucine and glutamine may regulate AMPK activities via alteration of the ATP/AMP ratio as well as an increase in Ca⁺⁺ influx.

1.5 Cellular effects of AMPK

1.5.1 AMPK mediates glucose transport in muscle

Muscle contraction activates AMPK, and the activated kinase enhances glucose uptake in skeletal muscle by causing the translocation of glucose transporter 4 (GLUT4) to the plasma membrane [14]. However, it has been suggested that glucose transport induced during muscle contraction may not be totally controlled by AMPK. This was concluded after a study with α_1 - and α_2 -AMPK-subunit knock out mice, showed that glucose transport in the fast twitch muscle was reduced by only 40%. Similarly, Nielsen and colleagues [14] using transgenic mice in which either α_1 - or α_2 -AMPK was knocked out, found that neither the absence

of α_1 nor that of α_2 affected, in any way, glucose transport induced by muscle contraction.

1.5.2 AMPK involvement in the nitric oxide signaling system

Fryer *et al.* [35] suggested that glucose uptake stimulated by AMPK in muscle is mediated by nitric oxide synthase. They observed that AICAR activation of AMPK and increase of glucose transport across rat and mouse muscle cells was paralleled by the activation of nitric oxide synthase. The treatment of these cells with nitric oxide synthase inhibitors completely blocked the increase of glucose transport across the cell membrane. In the same study, an inhibitor of guanylate cyclase was also found to inhibit AICAR induced glucose transport across the cell membrane. It is, therefore, likely that AMPK increases glucose transport in a pathway involving nitric oxide synthase and guanylate cyclase.

A study on the effects of a 30 second bicycle sprint exercise on AMPK activities [36], conducted on 7 males and 4 females of average age 22 ± 1.6 years, showed that this exercise induced the activation of both AMPK- α_1 and AMPK- α_2 . AMPK activation was paralleled by a rise of about 5,5 fold in the phosphorylation of neural nitric oxide synthase- μ (nNOS μ) at serine 145. However, this study was unable to show a direct association between nNOS μ activation and the increase in AMPK

activities. The activation of nNOS μ in response to intense exercise is believed to have a protective effect in muscle against ischemia and metabolic stress. Nitric oxide (NO) regulates muscle contraction, respiration in the mitochondria, glucose transport across the cell membrane, and neuromuscular transmission. Blood flow at rest and during recovery from exercise may also be regulated by NO [36]. AMPK is reported to phosphorylate and activate endothelial nitric oxide synthase (eNOS) in rat heart muscle in response to ischemia [36]. It is worth noting that ischemic conditions increase glucose uptake in the heart [36].

1.5.3 Role of AMPK in the regulation of the sympathetic nervous system

It is possible that AMPK plays a role in the functioning of the sympathetic nervous system. Viollet and colleagues [37] observed that AMPK $_{\alpha 2}^{-/-}$ transgenic mice have many metabolic defects, including insulin resistance, while their isolated organs are metabolically normal. AMPK $_{\alpha 2}$ is significantly expressed in neurons and activated astrocytes. The AMPK $_{\alpha 2}^{-/-}$ mice also had high levels of catecholamine, reduced insulin-stimulated glucose uptake in skeletal muscle, altered glycogen synthesis and a considerable increase in 24 hours urinary excretion, an effect associated with a chronic sympathetic activation.

1.5.4 AMPK may regulate gene expression

The activation of AMPK in pancreatic β -cells by a shift to low glucose or by treatment with AICAR, results in the reduction of expression of many important genes including glucose transporter 2 (GLUT2), aldolase B and liver-type pyruvate kinase (L-PK) [6]. In hepatocytes and hepatoma cell lines, AMPK activation by AICAR led to a decreased expression of fatty acid synthase (FAS), phosphoenolpyruvate carboxykinase (PEPCK), and glucose-6-phosphatase (G-6-pase) [6].

AMPK may control gene expression by directly phosphorylating transcription factors, transcription co-activators, or proteins involved in the transcriptional machinery. This assumption is supported by the fact that the yeast homologue of AMPK, sucrose non-fermenting 1 (Snf1), regulates gene expression in response to glucose availability by phosphorylating transcription factors. The transcription factor HNF4 is involved in the regulation of gene expression in the liver, intestine and pancreas [6]. Treatment of primary hepatocytes with AICAR resulted in a down-regulation of several HNF4 target genes, due to a decrease in HNF4 levels. AMPK may control HNF4 activity by phosphorylating it and enhancing its degradation [6]. AMPK is also believed to up-regulate the expression of transcription co-activators such as peroxisome proliferator-activated receptor coactivator 1 ($\text{PGC1}\alpha$) which plays a role in the expression of mitochondrial genes in muscle [2]. Another

role of AMPK in muscle gene expression is to increase the DNA binding activities of muscle transcription factors nuclear respiratory factor 1 (NRF1) and mesoderm/mesenchyme forkhead 2 (MF2). MF2 regulates the expression of glucose transporter 4 (GLUT4) [2].

The activation of AMPK was also observed to reduce the activity of RNA polymerase I, the polymerase that catalyses the transcription of rRNA [6]. AMPK regulation of gene expression can also take place at the level of translation. AMPK can inhibit gene translation by phosphorylating and activating the elongation factor-2 kinase which inhibits protein synthesis [2].

1.5.5 AMPK inhibition of intracellular lipid accumulation

A study by Habinowsky and Witters [25], conducted in mouse adipocytes showed a link between AMPK activation and lipid metabolism. Zang and colleagues [38] using metformin in hepatocytes, observed that AMPK activation by metformin was paralleled by a decrease in intracellular triacylglycerol and cholesterol.

Villena and colleagues [39], investigating the rate of adipose tissue formation in AMPK α_2 knockout mice compared to their wild type counterparts, found that knockout mice exhibited increased body weight and fat mass. This increase was caused by the enlargement of the pre-existing adipocytes and an increase in the rate of lipid

accumulation. These investigators also observed that there was no change in the expression of genes that control adipogenesis, such as CCAAT/enhancer-binding protein α (C/EBP α), peroxisome proliferator-activated receptor γ (PPAR γ), and adipocyte fatty acid binding protein (aFABP/aP2), in the knockout mice. This suggested that the increase in fat deposits in these mice was not due to an increase in the rate of proliferation of fat cells in the absence of AMPK- α_2 , but an increase in the accumulation of triglyceride.

Intracellular degradation of triglyceride is mainly achieved via the β -adrenergic pathway, where an increase in cAMP leads to the phosphorylation of hormone sensitive lipase (HSL) by protein kinase A (PKA). The phosphorylated HSL translocates to the lipid droplet to initiate triglyceride degradation. A study by Yin *et al.* [40] showed that AMPK activation by the β -adrenergic agonists isoproterenol, and forskolin, induces lipolysis in 3T3-L1 cells. AMPK activation by these two agents is believed to be mediated by an increase in the intracellular concentration of cAMP. AMPK may also phosphorylate HSL at Ser565, a phosphorylation that is associated with HSL translocation to the lipid droplet.

1.6 AMPK AND TYPE 2 DIABETES MELLITUS

Type 2 diabetes mellitus (T2DM) is becoming one of the leading health threats of the 21st century. The past few years have seen an alarming increase in the number of people diagnosed with diabetes throughout the world. Dramatic changes in our society resulting from globalization and industrialization, with their accompanying change in human behavior and life style are amongst the main causes behind the escalating rates of obesity and diabetes worldwide [41]. Beside environmental factors, the combination of heterogeneous genetic defects also plays an important role in determining susceptibility to T2DM. The close association of T2DM with genetic defects is supported by the fact that more than 90 % of identical twins are concordant for T2DM [42], and first degree relatives of diabetic persons have a 40 % chance of contracting T2DM compared with a 10 % chance in subjects with no family history of diabetes [43].

T2DM results from a combination of insulin resistance (reduced ability of insulin- sensitive tissues to respond to the binding of insulin to its receptor) and reduced pancreatic islet β -cell insulin secretion [44]. One of the major causes of insulin resistance is obesity [45]. Subjects who develop T2DM are those in whom the insulin output of the β -cells is not sufficient to counteract the insulin resistance, leading to hyperglycaemia and eventual β -cell secretory failure. The cause of the β -

cell failure in T2DM is not fully understood but possible candidates include glucotoxicity, lipotoxicity, low β -cell numbers and genetically programmed β -cell dysfunction [44].

1.6.1 Obesity and insulin resistance

Obesity is caused by an increased adipose tissue mass, resulting from proliferation (hyperplasia) and growth (hypertrophy) of adipocytes and adipocyte precursor cells [45]. The hypertrophy is due to increased intracellular levels of triacylglycerol (triglyceride) derived from dietary intake.

Adipose tissue functions like an endocrine organ in its regulation of body metabolism, by secreting hormones like adiponectin [45] and leptin [46]. Both these hormones are activators of AMPK. Adipose tissue also plays a critical role of preventing lipid accumulation in other tissues which can result in lipotoxicity [45]. Lipid accumulation in β -cells may cause β -cell dysfunction whilst its accumulation in muscle may lead to insulin resistance [45]. Lipid accumulation in both these tissues is increased in obese subjects.

Adipocytes secrete a number of factors that may affect insulin sensitivity. Prominent amongst these are $\text{TNF}\alpha$, interleukin 6 (IL6), free fatty acids (FFA) and adiponectin. $\text{TNF}\alpha$ interferes with insulin receptor kinase activity, while elevated FFA may cause hyperglycemia by inhibiting skeletal muscle

glucose uptake or by interfering with the ability of insulin to suppress hepatic glucose output, as well as decreasing glucose oxidation in muscle [47, 48]. Adiponectin increases insulin sensitivity but serum levels of this hormone fall with increasing body fat mass, via an unknown mechanism [49]. Recently, two new adipocyte derived factors, visfatin and vaspin have been discovered and shown to increase insulin sensitivity [50, 51].

1.6.2 The possible role of AMPK in the aetiology of type 2 diabetes

AMPK inhibition of diacyl and triacylglycerol formation may be one of the principal mechanisms by which AMPK activators such as metformin improve insulin sensitivity in skeletal muscle and other tissues [16].

AMPK activation inhibits the incorporation of fatty acids into glycerolipids, by inhibiting sn-glycerophosphate acyltransferase, an enzyme involved in diacylglycerol and triglyceride synthesis [52].

High glucose concentrations stimulate insulin secretion by the β -cells of the pancreas in two phases. The first phase is the release of insulin stored in the secretory vesicles, docked at the plasma membrane, into the blood stream. The second phase is the translocation of secretory granules from the endoplasmic reticulum to the plasma membrane of the cell. The movement of secretory granules is facilitated by microtubular motor proteins [3]. AMPK activation has been suggested to

inhibit the second phase of insulin secretion by phosphorylation of microtubular motor proteins [3]. Therefore, although AMPK actions on lipid metabolism may have beneficiary effects on insulin sensitivity, AMPK may be directly involved in the inhibition of insulin secretion in β -cells. It is also noteworthy that metabolisable amino acids such as leucine and glutamine, which stimulate insulin secretion, inhibit AMPK [3].

Steinberg and colleagues [53] conducted a study on the level of activation of AMPK and its downstream enzymes in muscle of obese and lean females. Their study revealed that AMPK mRNA expression, AMPK- α_1 and AMPK- α_2 activities, phosphorylation of acetyl-CoA carboxylase- β isoform (ACC- β), and the oxidation of fatty acids were similar in both lean and obese subjects. Most importantly they showed that AMPK could be activated by AICAR to a similar degree in both groups. The only difference, in the two groups being that leptin did not stimulate fatty acid oxidation in obese subject's skeletal muscle.

Musi *et al.* [54] compared the level of AMPK activation in muscle of type 2 diabetes and healthy subjects. They found that AMPK activation after 20 to 45 minutes of exercise, and 30 minutes post-exercise was the same in both groups. Musi and colleagues observed an increase in AMPK activation of about 2.7 fold from basal level in the two groups after exercise. However, the activation of AMPK was paralleled by a marked decrease in blood glucose concentration, from 7.6 to 4.77

mmol/L in the type 2 diabetic subjects, while the blood glucose concentration in the control group remained the same.

This reinforces the view that the AMPK pathway can be an attractive approach for improving glucose uptake in muscle of people suffering from type 2 diabetes or those affected by insulin resistance. Supporting this is the finding that AICAR increases glucose disposal in muscle and decreases blood glucose concentrations in animal models of diabetes [54].

The findings of Musi *et al.* [54] and Steinberg *et al.* [53] challenged suggestions that defects in the AMPK signaling pathway are implicated in the metabolic dysregulation observed in type 2 diabetes. However, there is growing evidence that counters this argument. Thus, AMPK defects have been linked with impaired insulin induced non-oxidative glucose metabolism, and impaired activation of glycogen synthase in muscle of obese subjects with type 2 diabetes [55]. Also in AMPK- α_2 knock out mice insulin resistance is observed and is due to effects on the central nervous system [55].

1.7 AMPK and HIV-1 replication

Acquired immunodeficiency syndrome (AIDS) is caused by the human immunodeficiency virus (HIV), which progressively kills cells of the immune system, therefore, destroying the body's ability to fight

infections and certain cancers. HIV is a member of the *retroviridae* family of virus (commonly known as retrovirus), and classified in the subfamily lentiviruses (slow viruses) [56]. It is widely accepted that HIV in humans originated from cross species transfer of a simian immunodeficiency virus (SIV) from chimpanzee, *pan troglodytes troglodytes* in central Africa, probably at the beginning of the 20th century [57]. HIV-1 and the closely related HIV-2, mostly found in West Africa, are believed to share a common ancestry. At the end of 2002 about 42 million adults and children were infected with HIV [58]. In 2002 it was estimated that 29.4 million HIV infected individuals lived in Sub-Saharan Africa and about 12% of the adult population in South-Africa is infected with the virus [59]. It is estimated that about 1 million people die every year of HIV related illnesses [60].

1.7.1 HIV-1 classification

HIV-1 is classified into four groups. The first group is the group M (major) which is further divided into clades also known as subtypes. The subtypes are labeled from A to D and from F to K [58, 59]. The recombinant group is made of viruses that are genomic recombinants of different subtypes of group M [59]. The recombinant viruses are very common in regions where there is circulation of different HIV-1 subtypes. HIV-1 group O (outlier) is largely restricted to the central African region

[59]. Lastly, group N (non-M, non-O) has been identified in very few cases of HIV-1 infection in Cameroon, Gabon, and France [59].

1.7.2 HIV-1 structure and life cycle

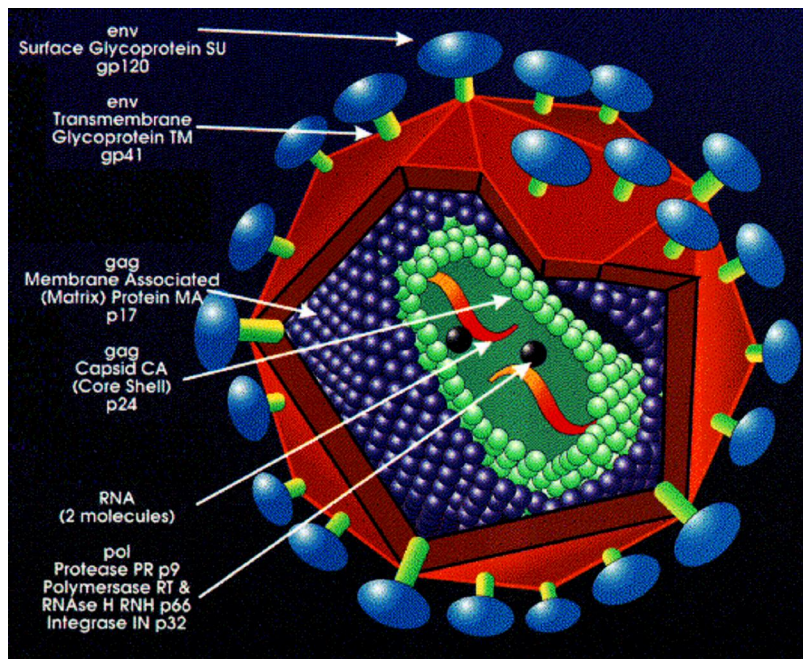


Figure 1.4: Diagram depicting HIV-1 outer proteins gp120 and gp41, and inner proteins p9, p17, p24, p32, and p66; the viral RNA genome, and the outer membrane lipid in brown [61].

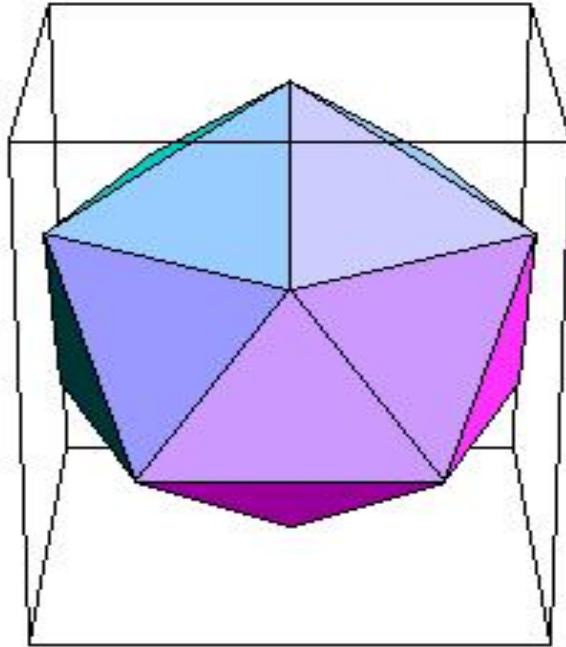


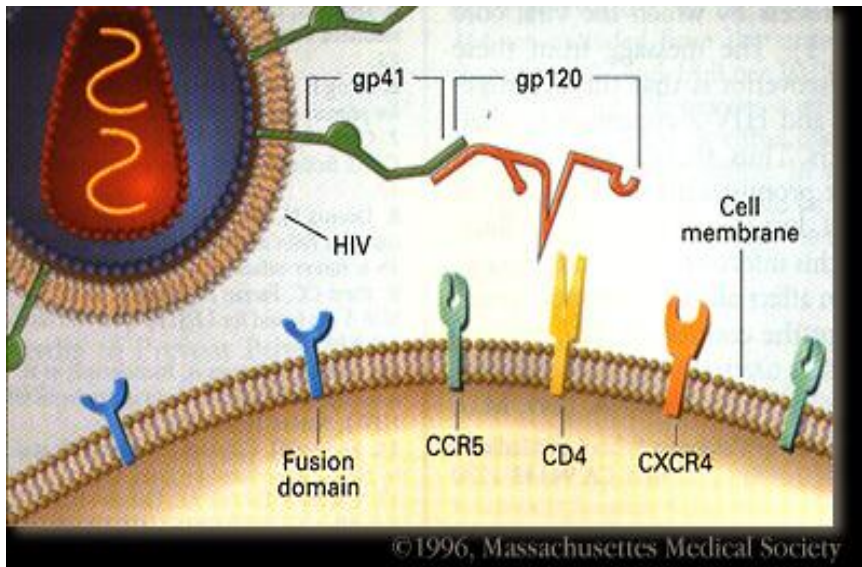
Figure 1.5: HIV-1 capsid, the structure inside the cube, has a roughly icosahedral structure [61].

The human immunodeficiency virus type 1 (HIV-1) has an RNA genome that replicates via a DNA intermediate once the virus is inside the target cell. The viral RNA genome is made of two identical copies of positive sense RNA, which together form a single-stranded mRNA of about 9,500 nucleotides long (figure 1.4). HIV-1 genomic RNA is found in association with the nucleocapsid protein p9 and p6. The viral genetic material, as

well as viral integrase and reverse transcriptase are contained in a capsid made of HIV-1 protein p24 (figures 1.4 and 1.5). The capsid is coated with a layer of matrix protein p17, which in turn is associated with the outer lipid layer, or viral envelope, acquired from an infected cell. Out of the viral envelope protrude gp120 and gp41 proteins, which help the virus attach to the host cell receptors during infection (figure 1.6 (A) and (B)) [62].

In the host cell HIV-1 reverse transcriptase synthesizes a double-stranded DNA version of its RNA genome. The DNA is then integrated, as a provirus, into the host cell genome. The provirus becomes part of the host cell DNA and it is replicated along with it, every time the cell divides. Two identical structures, the long terminal repeat (LTR), are generated at each end of the provirus, in the course of the reverse transcription of the HIV-1 genomic RNA. During the course of an HIV infection the transcription of the integrated provirus begins with the activation of enhancer and promoter sequences in the LTR (figure 1.7) [63].

A.



B.

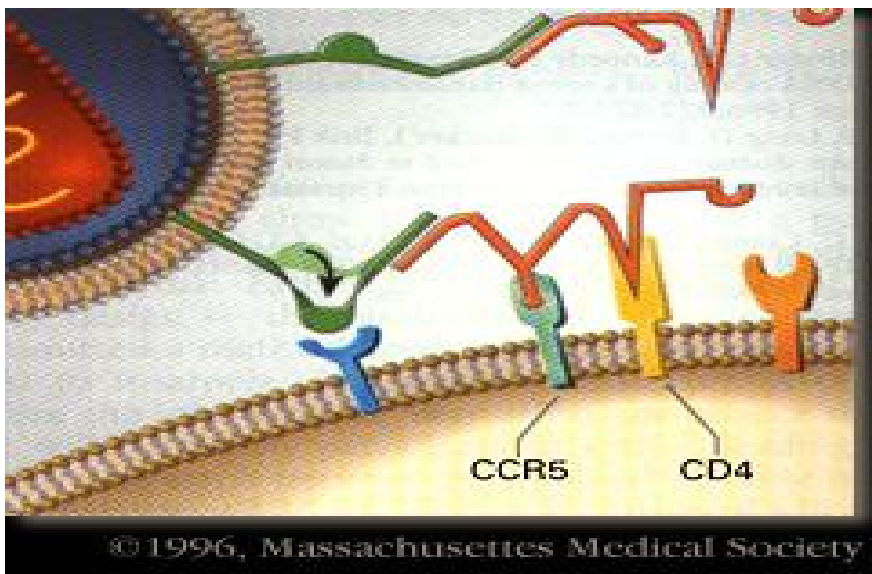


Figure 1.6: (A) and (B) Show the interaction of HIV-1 gp120 and gp41 with the host cell receptor CD4 and co-receptor CCR5 [62].

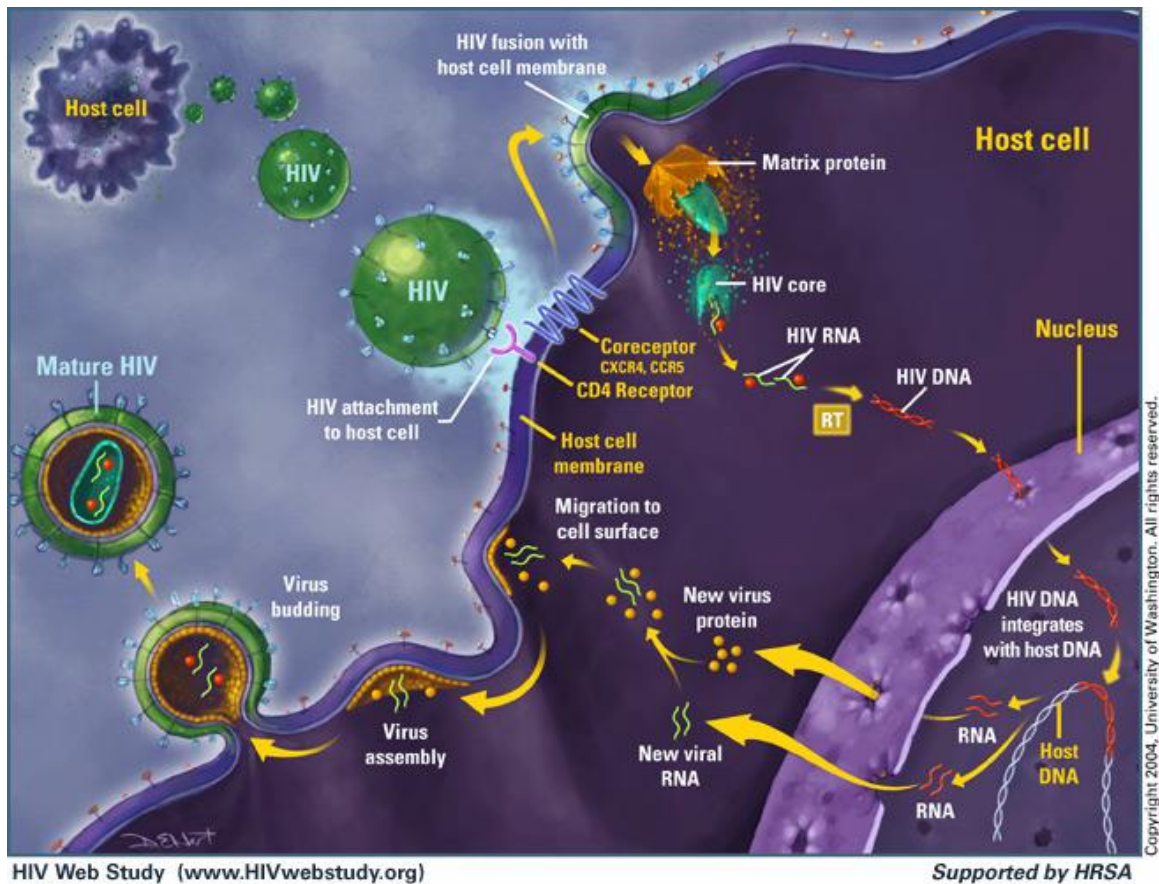


Figure 1.7: Diagrammatic representation of HIV-1 life cycle [61].

1.7.3 HIV-1 infectivity

Many cellular factors can promote HIV-1 replication in a latently infected cell i.e. in an infected cell that does not produce viral particles. These factors may include antigens which can stimulate the differentiation of infected cells, therefore, stimulating the integrated provirus to replicate. The infection of the host cell by other viruses such as the herpes

simplex virus or the cytomegalovirus may also result in the initiation of viral replication [58]. HIV-1 transcription results in the production of infective virions that will bud from the host cell into the blood stream to infect other target cells. HIV-1 targets cells carrying the CD4 cell surface antigen and the chemokine receptors CCR5 and CXCR4 are also required for a successful infection (figure 1.6 (A) and (B)) [64]. HIV-1 infects mainly T-cells (figure 1.8), monocytes, macrophages, and dendritic cells. However, except for T-cells, the other cells are generally not destroyed by HIV-1; they act as a viral reservoir in an infected individual [7].



Figure 1.8: A photograph of HIV, in blue, budding from a T-cell [65].

1.7.4 HIV-1 genome

The HIV-1 genome contains 9 genes [57]. The *env* encodes the viral protein gp160 the precursor protein of gp120 and gp41; the *gag* gene product is the precursor polyprotein Pr55 which is cut by HIV-1 protease to make 4 small internal structural proteins [66]. The role of *Nef* is still uncertain; however, it is believed that it may play a role in the infection of the host cell. *Pol* encodes the polyprotein Pr160, the precursor of HIV protease and reverse transcriptase [66]. *Rev* encodes HIV-1 Rev protein which plays the role of transferring viral RNA from the nucleus into the cytoplasm [67]. *Tat* encodes Tat which increases the rate of expression of HIV-1 genes [68]. *Vif* increases HIV-1 infectivity; *vpr* encodes transcriptional activators and *vpu* participates in viral assembly and budding [66].

1.7.5 Nuclear factor- κ B and HIV-1 replication

The NF- κ B proteins are a large family of inducible nuclear factors responsible for controlling gene expression after injury or during the inflammatory response [69]. Proteins of this family share a conserved 300 amino acid region called Rel homology domain (RHD), responsible for DNA binding and dimerization. So far eight members of the NF- κ B family have been identified: NF- κ B1 (p50/p105), NF- κ B2 (p52/p100),

cRel, RelA (p65), RelB and the drosophila proteins Dorsal, Dif and Relish. P50 and p52 are generated by proteolytic processing of p105 and p100, respectively [69, 70]. The most abundant member of the family, however, is a heterodimer made of subunit p50 and p65 (figure 1.9). P65 contains a powerful transcriptional activation domain. NF- κ B dimers are found in their inactive form in the cytoplasm where they are bound to one of 3 inhibitor I κ B isoforms (I κ B α , I κ B β , and I κ B ϵ) [71]. Physiological factors, such as interleukin-1 and tumor necrosis factor (TNF)- α , can induce the phosphorylation of I κ B by I κ B kinase (IKK) β . The phosphorylated I κ B is ubiquitinated and degraded by the 26S proteasome. This releases NF- κ B allowing it to migrate to the nucleus to bind to DNA and initiate gene transcription (figure 1.10). In addition to the classical NF- κ B cascade, another pathway to generate a different NF- κ B complex (RelB attached to p100) has been proposed. This pathway involves IKK α , a subunit of the IKK complex, rather than IKK β . IKK α phosphorylates p100, in the cytoplasm, and this triggers processing of p100 to p52. The activated RelB-p52 complex then migrates to the nucleus to induce gene transcription [70]. Phosphorylation is extensively involved in the metabolic control of NF- κ B activities i.e. its transport to the nucleus, processing of its precursors, stabilization of its dimeric form, and its binding to DNA. In the nucleus phosphorylation of p65 by mitogen- and stress-activated protein kinase-1 (MSK-1) at residue Ser276 of the RHD region, in response to TNF- α ,

induces NF- κ B-dependent gene transcription. P65 is also phosphorylated by protein kinase A (PKA) [70] leading to increased transcription of NF- κ B responsive genes.

It is possible that NF- κ B induces gene transcription by combining with other nuclear proteins, such as CBP/p300, via the p65 subunit. Mutation at Ser276 blocks NF- κ B binding to CBP/p300 and results in the loss of NF- κ B induced gene transcription [69].

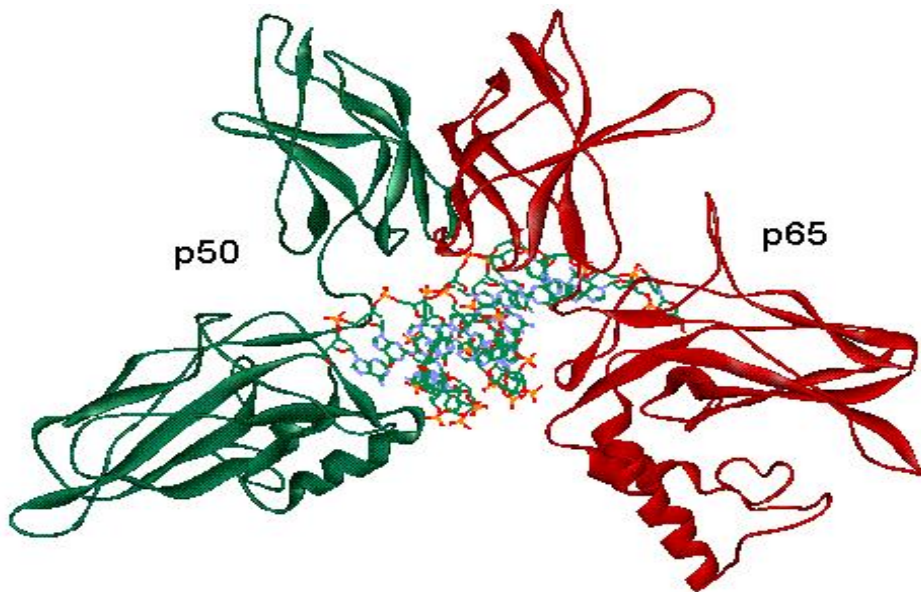


Figure 1.9: Chemical model of the most abundant member of the NF- κ B family [72].

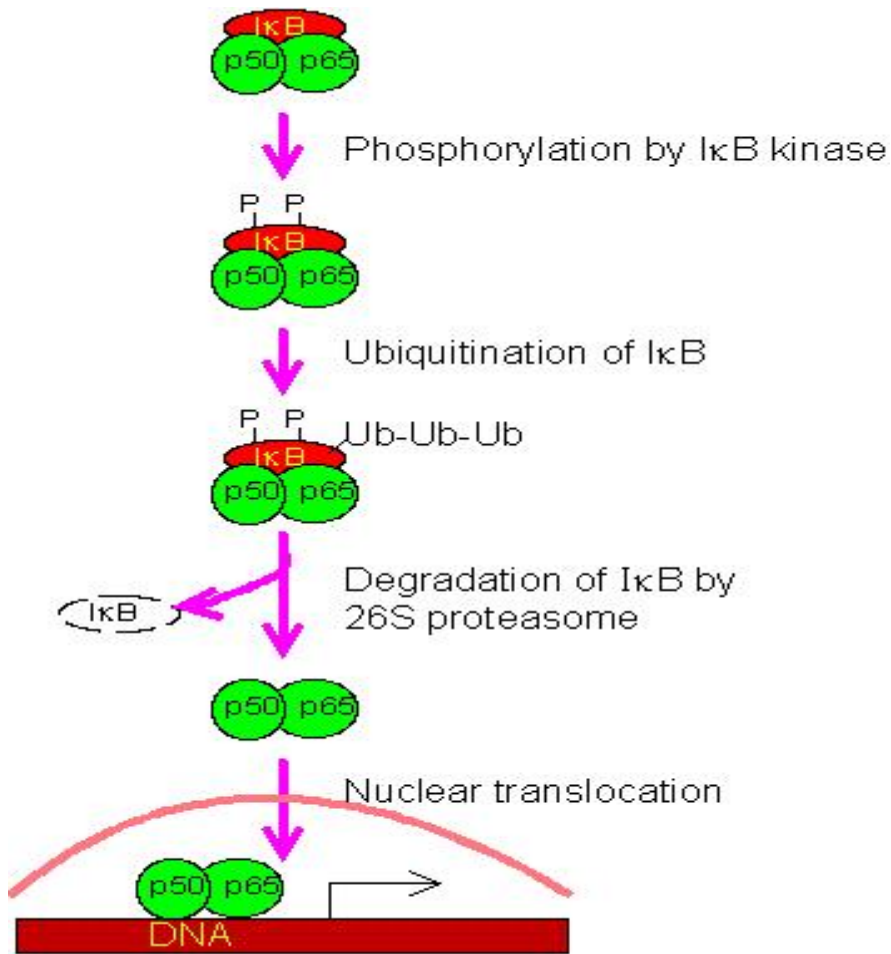


Figure 1.10: IκB phosphorylation and degradation followed by NF-κB release and migration to the nucleus, where it initiates gene transcription [72].

1.7.6 NF- κ B cooperates with the viral protein Tat to initiate HIV-1 replication

The replication of HIV-1 in T-lymphocytes is modulated by the viral proteins *Tat*, *Rev* and *Nef*. *Tat* and *Rev* bind to the viral RNA transcript, and are essential for gene expression at the transcriptional and posttranscriptional levels. In addition to these proteins, there is a strong requirement for host cell factors before HIV-1 replication begins [63].

The long terminal repeat in the viral genome regulates gene expression.

HIV-1 LTR is divided into three main regions: modulator, core and TAR.

The modulator region contains numerous cis-acting sequences for the binding of transcriptional factors such as NF- κ B, NF-AT and AP-1. These cis-acting sequences have two highly conserved copies of the κ B elements. The activation of the κ B element is achieved by the binding of an activated NF- κ B.

Cheng *et al.* [63] studying the activation of the HIV-1 genome by the human T-cell leukemia virus type-1 Tax protein showed that the activation of HIV-1 LTR by Tax is achieved through cooperation of this protein with HIV-1 *Tat*. Most importantly, they observed that the activation of a mutant strain of HIV-1 that had a deletion in the κ B element was reduced about 145-fold compared to the wild type. Using nuclear factor activators such as phorbol myristate acetate (PMA) for NF- κ B and phytohemagglutinin (PHA) for NF-AT, these investigators came to

the conclusion that NF- κ B was required for full activity of the HIV-1 LTR and that this nuclear factor was critical for *Tat* responsiveness, especially during the early postintegration stage of HIV-1 infection [63]. The same study also showed that the HIV-1 *Nef* protein activates viral replication in association with *tat* and NF- κ B. It is worth noting that a latent viral infection is in part maintained by the lack of cellular transcription factors, needed for the induction of HIV early regulatory genes [7]. Herpes simplex virus infection of HIV-1 infected cells, as well, appears to activate HIV-1 LTR expression partly through the activation of NF- κ B binding activities [73].

1.7.7 NF- κ B cis-acting motifs regulate HIV-1 transcription in human macrophages

Macrophages play an important role during the sexual transmission of HIV-1, as this mode of transmission involves mucosal tissues where macrophages are amongst the first cells to be exposed to the virus. At the early stages of an HIV-1 infection the viral strains found in the system are macrophage tropic and T-lymphocyte tropic viruses emerge progressively as the disease progresses [64].

Macrophages contain a constitutive nuclear pool of NF- κ B and in contrast to T-cells this pool allows for a basal level of HIV-1 transcription and replication in the absence of cell stimulation. The

ability of HIV-1 to infect and replicate in macrophages is critical to the pathogenesis of AIDS. Macrophages behave like major viral reservoirs, facilitating persistent HIV-1 replication and infection of target cells via cell to cell contact, hence, accelerating the progression to AIDS [7]. Asin and colleagues [7] investigating the role of the nuclear pool of NF- κ B in HIV-1 transcription, observed that its inhibition with a dominant NF- κ B inhibitor, I κ B α , led to a significant reduction of HIV-1 replication in the promonocytic U937 cell line. The reduction of this pool in human macrophages by an adenovirus vector expressing a dominant negative I κ B α also gave the same result [7].

A study by Paya *et al.* [74] showed that HIV-1 infected U937 cells, had an increased accumulation of NF- κ B (p50/p65) in their cytoplasm when compared to uninfected U937 cells. It is believed that HIV-1 infection of U937 results in a continuous translocation of NF- κ B (p50/p65) to the nucleus. The translocated NF- κ B up-regulates the gene expression of p105, precursor of p50. This in turn causes p50/p65 NF- κ B accumulation in the cytoplasm. The observation that HIV-1 may perpetuate its own gene transcription in monocytes may explain why macrophages play the role of viral reservoirs during an HIV-1 infection.

1.7.8 TNF- α initiate HIV-1 replication via NF- κ B

Duh *et al.* [73] using a chronically infected T-cell line (ACH 2), observed that its treatment with TNF- α results in an increase in the steady-state level of HIV-1 RNA and HIV-1 transcription. They observed a 4- to 5- fold increase in steady-state HIV-1 RNA and a 3- fold increase in HIV-1 transcription. This occurred through a transcriptional activation of the HIV-1 long terminal repeat (LTR) and binding of a nuclear factor to the NF- κ B sites. It is interesting to note that there is an increase in the plasma level of TNF- α in AIDS patients compared to asymptomatic HIV-seropositive individuals [73] .

1.7.9 AMPK inhibition of transcriptional activators used by HIV-1

It can be concluded that NF- κ B (p50/p65) is a key nuclear factor that promotes HIV-1 gene expression. Interestingly, AMPK activation by AICAR suppresses NF- κ B mediated gene expression [1]. Similarly, adiponectin, an abundant adipocyte-derived plasma protein and a well known activator of AMPK, inhibits TNF- α induced expression of adhesion molecules on cultured endothelial cells. This is caused by adiponectin inhibition of TNF- α mediated phosphorylation of inhibitor- κ B (I- κ B), leading to inactivation of NF- κ B [75].

AMPK has also been reported to phosphorylate the transcriptional co-activator p300 and CBP. The phosphorylation of p300 inhibits its interaction with nuclear receptors, while CBP phosphorylation blocks its binding to DNA [1]. As shown by Marzio *et al.* [76] p300 and CBP, which have histone acyltransferase activities and are required for the initiation of HIV-1 replication, are recruited by HIV-1 *tat* at the viral LTR before the initiation of gene transcription. Also as said earlier NF- κ B p65 interacts with p300/CBP during gene transcription [69].

1.7.10 HIV treatment

The first anti-retroviral approved for use against HIV is zidovudine, also known as AZT. This drug was first developed as an anti-cancer; however, in late 1980s it became known that AZT also had anti-retroviral activities [77]. AZT is a nucleoside analogue reverse transcriptase inhibitor (NRTI), it inhibits HIV reverse transcriptase [77]. Besides AZT other NRTI such as didanosine and zalcitabine are also used against HIV [77]. HIV infection can also be treated with Non-nucleoside analogue reverse transcriptase inhibitors (NNRTI) such as efavirenz and protease inhibitors (PI) such as indicavir [77]. However, the most effective treatment of HIV infection is the highly active anti-retroviral therapy (HAART). This treatment combines at least 3 anti-retroviral drugs in a single regimen.

Long term HAART have been associated with severe side effects amongst which are lipodystrophy, insulin resistance and type 2 diabetes, cumulative mitochondrial damage, and lactic acidosis [77]. The treatment of HIV infection with single NRTI, NNRTI, or PI has also been associated with toxic effects ranging from mild to life threatening [77].

1.8 Aims of the study

Metformin is known to cause weight loss. Metformin and AICAR can activate AMPK, and AMPK activation in pre-adipocytes causes an inhibition of adipogenesis. Therefore, the first aim of this study was to investigate whether metformin may inhibit adipogenesis in the murine pre-adipocytes cell line 3T3-L1. The second objective was to study metformin and AICAR activation of AMPK and to determine if this inhibits HIV-1 replication in chronically infected U1-cells, by inhibiting NF- κ B expression.

CHAPTER 2

MATERIALS AND METHODS

2.1 AMPK inhibition of adipogenesis

2.1.1 Optimization of AICAR and metformin concentration for adipogenesis

The optimization experiment was performed with 0.5 mM, 0.75 mM, and 1 mM AICAR (see appendix II for the preparation of AICAR stock solution). The choice to use 1 mM as the highest concentration of AICAR in the titration curve was based on Hawbinosky and Witters study [25] on AICAR inhibition of adipogenesis in 3T3-L1, mouse pre-adipocytes that can be transformed into adipocytes. In this study the inhibition of adipocyte differentiation was the highest in cells cultured with 1 mM AICAR.

The optimization experiment for metformin began with 2 mM (see appendix II for the preparation of metformin stock solution). The other two concentrations used were 3 mM and 4 mM. The choice to begin the titration curve with 2 mM was based on a Zhou *et al.* study [9] that used the same concentration of metformin to inhibit intracellular lipid accumulation in hepatocytes.

The method used for the optimization experiment was as follows:

1. The 3T3-L1 cell line (appendix I) was cultured in DMEM maintenance medium (appendix II) in a 25 cm² flask, at 37 °C in a humidified atmosphere containing 5 % CO₂.

2. At confluence cells were trypsinized (section 2.1.4) and a 0.5 mL aliquot was transferred to eight 25 cm² flasks.
3. These cells were cultured to confluence.
4. At confluence (day 0) one tissue culture was stained with Oil red O [78] for baseline lipid content.
5. For the remaining seven flasks (on day 0): one culture was left untreated (the negative control), three were treated with different concentrations of metformin, 2 mM, 3 mM, and 4 mM; and three others were treated with 0.5 mM, 0.75 mM, and 1 mM AICAR and cell transformation (adipogenesis) was induced in these seven tissue cultures by treating the cells in 5 mL of maintenance medium with 5×10^{-4} M 3-isobutyl-1-methylxanthine (IBMX), 2.4×10^{-7} M dexamethasone and 0.28 U/mL insulin (see appendix II for the preparation of IBMX and dexamethasone stock solutions).
6. On day three the medium was changed to maintenance medium plus insulin only.
7. On day six the culture medium was replaced with maintenance medium without IBMX, dexamethasone, or insulin, until day eight.
8. On day eight all the cultures were stained with Oil red O (section 2.1.6).

2.1.2 3T3-L1 cell culture, treatment with AICAR and metformin, and initiation of adipogenesis

The initiation of adipogenesis of cells treated with AICAR and metformin was carried out as described in section 2.1.1. In this experiment cells were treated with 2 mM, 4 mM, 8 mM, and 16 mM of metformin. Cells treated with 1 mM of AICAR were used as positive control, as AICAR is a well known inhibitor of adipogenesis [25].

2.1.3 Detection of AMPK phosphorylation by AICAR and metformin

1. 3T3-L1 cells were cultured in a 25 cm² flask as in section 2.1.1.
2. At confluence cells were trypsinized and a 0.5 mL aliquot was transferred to four 25 cm² flasks.
3. Cells were again cultured until confluent.
4. At confluence, total cytoplasmic protein was extracted from one culture (section 2.1.7), for Western blotting to quantify the baseline phosphorylation of AMPK (section 2.3).
5. For the remaining three flasks: one culture was left untreated, one culture was treated with 16 mM metformin; and the last cell culture was treated with 1 mM of AICAR and cell transformation was induced in these three cultures using the method described in section 2.1.1.

6. After three days the medium was changed to maintenance medium plus insulin only.
7. On day six the culture medium was replaced with a maintenance medium without IBMX, dexamethasone, or insulin, until day eight.
8. On day eight total cytoplasmic protein was extracted from all the cultures, and Western blotting was performed (section 2.3), to measure the phosphorylation of AMPK by AICAR and metformin. This experiment was repeated five times.

2.1.4 3T3-L1 trypsinization

1. Confluent 3T3-L1 cells in a 25 cm² flask were trypsinized by washing the cells twice with phosphate-buffered saline (PBS) (appendix II), 5 mL for the first wash and 1 mL for the second.
2. PBS was pipetted out of the flask and the cells were left in 1 mL trypsin for 10 to 15 minutes at 37 °C.
3. The trypsinization reaction was stopped by adding 4 mL of maintenance medium into the flask.
4. Suspended cells were then transferred to the relevant number of fresh flasks, containing maintenance medium, for tissue culture.

2.1.5 Oil red O preparation

1. Oil red O (105 mg) was dissolved in 30 mL of absolute isopropyl alcohol. The solution was stirred overnight on a magnetic stirrer, at room temperature.
2. The following day the solution was filtered thrice through a Whatman paper filter, and 22.5 mL of bidistilled water was added to the solution.
3. The solution was left at 4 °C overnight, for use the following day.

2.1.6 Oil red O staining

When 3T3-L1 cells are stained with Oil red O, the dye enters the cells and binds to intracellular lipid. Therefore, the higher the concentration of lipid inside the cell, the higher the amount of dye that binds to them. The dye is then extracted with 60 % (v/v) isopropyl alcohol in water and the absorbance readings of the dye-isopropyl alcohol solution is taken at 510 nm. The optical density is, therefore, proportional to the intracellular lipid concentration.

The method used was as follows:

1. 3T3-L1 cells in a 25 cm² flask were fixed with 2 mL of 3 % (v/v) gluteraldehyde in water for 2 hours.

2. The gluteraldehyde solution was poured out and replaced with 2.5 mL of 60 % (v/v) isopropyl alcohol.
3. After 5 minutes the 60 % isopropyl alcohol was removed from the flask, and the flask was left with its cap removed for ten minutes, to allow for residual isopropyl alcohol to evaporate.
4. The cells were stained with 1.5 mL Oil red O for 2 hours.
5. The dye was removed from the flask and the cells were rinsed with 2.5 mL of 60 % (v/v) isopropyl alcohol for 5 seconds.
6. The dye was extracted by adding 3.5 mL of 60 % (v/v) isopropyl alcohol and leaving the flask on an electric shaker for 2 hours.
7. The optical density of the extracted dye was read at 510 nm.

2.1.7 Protein extraction from 3T3-L1

1. Adherent 3T3-L1 cells were removed from culture flasks by treatment with trypsin.
2. The cells were pelleted by centrifugation at 670 xg for 10 minutes and resuspended in 5mL of warm Krebs-HEPES buffer (appendix II). The resuspended cells were left in the incubator for 30 minutes at 37°C.
3. Cells were again centrifuged at 670 xg for 10 minutes and the resulting pellet was kept on ice while 0.8 mL of ice-cold lysis buffer (appendix II) was added to it.

4. The cell lysate was centrifuged at 18,000 xg at 4 °C for 3 minutes and the resulting supernatant retained for Western blotting.
5. The protein concentration was determined using the Bradford method (section 2.1.8).

2.1.8 Determination of protein concentration using the Bradford Method

Required:

Coomassie reagent (appendix II),

albumin at a concentration of 1 mg/mL for standard curve [79].

The standard curve was prepared as follows:

Stock Albumin (μL)	H ₂ O	Concentration ($\mu\text{g/mL}$)
0	1000	0 (blank)
20	980	20
40	960	40
60	940	60
80	920	80
100	900	100

Method

1. Duplicate 5 mL tubes were labeled according to standards and samples.
2. 300 μ L standard/sample and 2.7 mL of coomassie reagent were added to each tube.
3. The sample and reagent were mixed and the absorbance reading was taken at 595 nm on a spectrophotometer.

Notes: Lysates from 10^6 cells should be diluted 1:20 as a starting point to fall within the standard curve.

2.2 AICAR and metformin inhibition of HIV-1 replication in U1 cells

2.2.1 Optimization of AICAR and metformin concentration for HIV-1 inhibition in U1 cells

Because this study was carried out after the adipogenesis study, the choice of AICAR and metformin concentrations to use against HIV-1 was guided by the concentrations used in the adipogenesis study i.e. for metformin we used the same concentrations we used in the adipogenesis study, except 2 mM, and for AICAR we used concentrations ranging from 0 to 1 mM.

The concentration of AICAR and metformin was optimized by using the following method:

1. U1 cells, HIV-1-chronically infected monocytes [80, 81], were cultured in suspension in a 75 cm² flask. The cells were grown in RPMI 1640 containing 10 % foetal calf serum, at 37 °C in a humidified atmosphere containing 5 % CO₂.
2. After 72 hours, viable cells were counted under an inverted light microscope using trypan blue exclusion. Viable cells stained light blue and non-viable cells stained dark blue. A 1×10⁶ cells/mL solution was prepared in RPMI 1640, supplemented with 10 % foetal calf serum.
3. A 0.5 mL aliquot was transferred into nine wells of a 24-well plate and cells were treated with 4 mM, 8 mM, and 16 mM metformin (the concentration of metformin stock solution is given in appendix II), in triplicate. In another 24 well plate U1 cells were treated with 0.1 mM, 0.2mM, 0.35mM, 0.4mM, 0.5mM, and 1mM of AICAR (the concentration of AICAR stock solution is given in appendix II), also in triplicate. In six wells of a third 24-well plate was transferred 0.5mL of the cell suspension. These remaining 6 wells remained untreated, these cells will be referred to as untreated cells.
4. The cell cultures were incubated for 1 hour at 37 °C to allow metformin and AICAR to activate AMPK.

5. HIV-1 replication was activated by the addition of NaCl to a final concentration of 60 mM [80] (the concentration of NaCl stock solution is given in appendix II) to metformin and AICAR treated wells, including three of the six untreated wells. Three untreated wells were used as the positive controls, and three untreated wells remained without AICAR, metformin, and NaCl and were used for background measurement of p24, HIV-1 core protein, in U1 cells.
6. After 48 hours, U1 cells in all the wells were counted using an inverted light microscope and HIV-1 replication was measured by measuring the p24 antigen concentration [80], of each culture, by ELISA. The p24 ELISA was performed on the supernatant from each well, according to the manufacturer's instructions (Dupont, Boston, MA) (section 2.2.3).

2.2.2 U1 cell culture and treatment with AICAR and metformin

This experiment was carried out the same as in section 2.2.1. However, the concentrations of AICAR used here were 0.2 mM, 0.35 mM, and 0.4 mM. Cells treated with 0.4 mM AICAR, 16 mM metformin, and cells treated with NaCl only, were used for the extraction of total nuclear and total cytoplasmic protein (section 2.2.4).

Western blotting (section 2.3) was performed with these protein extracts to quantify the cytoplasmic and nuclear concentrations of NF- κ B. The protein extracts were also used for the AMPK α subunit and phospho-AMPK α subunit Western blotting.

2.2.3 HIV-1 P24 antigen ELISA

The p24 ELISA uses a 96-well plate coated with anti-HIV-1 p24 antibody. HIV-1 replication results in the budding of the virus from the infected cell into the culture supernatant [82]. The amount of p24, after lysing the virus with Triton X 100®, captured on the plate is proportional to the rate of HIV-1 replication in the cells [80].

The rows of the plate were labeled from A to H, and the columns were labeled from 1 to 12.

The protocol was the following:

1. Serial dilutions for the standard curve were made, with the p24 antigen (provided), using row A to F of column 1, as follows:
A = 10.0 ng/mL of p24 (190 μ L of 0.5% Triton-X 100 + 10 μ L of p24 solution).
B = 2.5 ng/mL of p24 (150 μ L of 0.5% Triton-X 100 + 50 μ L of A).
C = 0.625 ng/mL (150 μ L of 0.5% Triton-X 100+ 50 μ L of B).
D = 0.156 ng/mL (150 μ L of 0.5% Triton-X 100+ 50 μ L of C).

E = 0.04 ng/mL (150 μ L of 0.5% Triton-X 100+ 50 μ L of D).

F = 0.01 ng/mL (150 μ L of 0.5% Triton-X 100+ 50 μ L of E).

Well G of column 1 was used as the blank for background reading.

2. 100 μ L of the sample was added to the ELISA plate. Note that the sample is 25 μ L of the U1 cell culture supernatant plus 225 μ L of 0.5% Triton-X 100.

After adding the sample to the plate, the plate was sealed and incubated for 1 hour at 37 °C. After the incubation the plate was washed 6 times and dried. All reagents, including the wash buffer, were supplied with the kit.

3. A 100 μ L aliquot of the detector antibody was added to all the wells except the blank. The plate was sealed and incubated for 1 hour at 37 °C. After the incubation the plate was washed 6 times and dried.

4. Streptavidin-HRP (horse radish peroxidase) was diluted 1:100 with Streptavidine-HRP diluent and 100 μ L of the streptavidine-HRP solution was added to all the wells except the blank. The plate was sealed and incubated at room temperature for 30 minutes, then washed 6 times and dried.

5. OPD: 1 tablet/11 mL of substrate diluent was prepared and 100 μ L of this solution added to all wells, including the blank.

6. Kinetic curve setting was used to read the optical density (OD).

From these values taken in a given interval of time i.e. the rate of

conversion of the substrate, the p24 concentration in different wells was calculated by the computer connected to the plate reader.

Note that all the concentration readings were multiplied by 10 as the samples were diluted 10 times (25 μ L of the U1 cell culture supernatant plus 225 μ L of 0.5% Triton-X 100).

2.2.4 U1 cell protein extraction

The Nucbuster protein extraction kit (appendix I) was used according to the manufacturer's instructions:

All extractions were performed on ice to enhance protein stability.

1. U1 cells were pelleted in a 1.5 mL Eppendorf tube by centrifugation at 500 xg at 4 °C. The supernatant was removed and 150 μ L of Nucbuster reagent 1 was added to the pellet.
2. The tube was vortexed for 15 seconds at high speed, incubated on ice for 5 minutes and again vortexed for 15 seconds at high speed.
3. The tube was centrifuged at 16,000 xg for 5 minutes at 4 °C.
4. The supernatant (cytoplasmic fraction) was stored at -20 °C.
5. The pellet was resuspended in a solution of 1 μ L of resuspended 100 X inhibitor cocktail, 1 μ L of 100 mM DDT, and 75 μ L NucBuster extraction reagent 2.

6. The pellet was vortexed for 15 seconds at high speed, incubated on ice for 5 minutes and again vortexed at high speed for 15 seconds.
7. The pellet was centrifuged at 16,000 xg for 5 minutes.
8. The supernatant (nuclear extract) was transferred to a separate tube and stored at -80 °C.

Protein concentration was determined using the Bradford method as described previously (section 2.1.8).

2.3 Western blotting

2.3.1 Protein electrophoresis

1. One part of the reducing solution with loading dye (appendix II) was mixed with 4 parts of the sample in a 1.5 mL Eppendorf tube.
2. The cap of the Eppendorf tube was pierced with a needle, and the tube was placed in a heating block at 70 °C for 5 minutes.
3. The heated solution was cooled and 4 µg of each protein extract was loaded onto a sodium dodecyl sulfate PAGE gel (appendix II).
4. The gel was run for 2 hours at 120 V (constant voltage) and a current of 63 mA.

2.3.2 Protein transfer to the Immobulon-P membrane

1. The gel was removed from its glass cassette, and the stacking gel was trimmed away.
2. The gel was equilibrated in the transfer buffer (appendix II) for 15 to 30 minutes.
3. Two Biorad trans-blot filter papers were soaked in the transfer buffer for at least 30 seconds. Four packing sponges of the same size as the filter papers and of about 3 mm thickness were soaked in the transfer buffer for at least 2 minutes. An Immobulon-P membrane (appendix I) was soaked in methanol for 15 seconds (The membrane should uniformly change from opaque to semi-transparent when soaked in methanol). The membrane was then carefully placed in ultra-pure water (milli-Q water) and soaked for 2 minutes. Finally the membrane was placed in the transfer buffer and equilibrated for at least 5 minutes.
4. A pre-soaked packing sponge was placed in the centre of the cathode half of a cassette holder.
5. A piece of wet filter paper was placed on the sponge. The equilibrated gel was placed on the filter paper.
6. The immobulon-P membrane was put on the gel. The membrane should not be re-positioned once it contacts the gel.

7. One piece of wet filter paper was placed on the membrane, and two or more packing sponges were put on top of the filter paper.
8. The cassette holder was closed and placed in the transfer tank.
9. The transfer buffer was poured into the cassette holder until it covered the cassette.
10. Cold distilled water was poured into the transfer tank, to absorb the heat released by the current used for protein transfer. The transfer was carried out using a constant current of 250 mA for 1 hour.

2.3.3 Drying the membrane after protein transfer

After the protein transfer, the membrane was dried by soaking it in 100 % methanol for 10 seconds, and by leaving it on a piece of filter paper at room temperature for approximately 15 minutes, until dry.

2.3.4 Rapid chemiluminescent detection of proteins on the Immobulon-P membrane

Rapid immunodetection takes advantage of the fact that antibodies cannot bind to the hydrophobic surface of the Immobulon-P membrane, but will bind to a protein immobilized on the membrane. With this detection method, blocking of the membrane is not required. Excess antibody cannot bind to a dry membrane and therefore reduces the amount of washing.

The membrane should be thoroughly dry for the detection to be successful.

1. The primary antibody (anti-phospho-AMPK₂ subunit, anti-AMPK₂ subunit, or anti-NF- κ B antibody) was prepared in 1% milk tris-buffered saline-tween20 (TBS-T) (0.1 % tween) (appendix II). The primary antibodies were diluted as follows: anti-phospho-AMPK₂ 1/1000, anti-AMPK₂ 1/1000, anti-NF- κ B 1/500.
2. The blot was placed in primary antibody solution and incubated with agitation for 1 hour.
3. The blot was rinsed quickly with TBS-T, and placed again in TBS-T and washed for 5 minutes. The washing was repeated twice with fresh buffer.
4. The blot was placed in the horse radish peroxidase (HRP)-conjugated secondary antibody solution, in 1 % milk TBS-T, and

incubated with agitation for 30 minutes. Note that the anti-phospho-AMPK₂ and the anti-NF- κ B were raised in rabbit; therefore, the secondary antibody used for their detection was a goat anti-rabbit antibody diluted 1/2000. Anti-AMPK₂ was raised in sheep; hence, the secondary antibody used for its detection was a rabbit anti-sheep diluted 1/1000.

5. The blot was rinsed quickly with TBS-T, and placed again in TBS-T and washed for 5 minutes. The washing was repeated twice with fresh buffer.
6. The substrate for enhanced chemiluminescent (ECL) (appendix I) detection was prepared by mixing an equal volume of ECL detection reagent solution 1 and ECL detection reagent solution 2.
7. The blot was placed in a container; a sufficient amount of the substrate was added to cover the entire surface of the membrane; and incubated for 1 minute.
8. The excess substrate was drained with a piece of paper towel.
9. The blot was placed on a clean piece of plastic wrap, protein side down, and wrapped.
10. Air bubbles, between the membrane and the plastic wrap, were removed by gently passing a finger across the surface of the plastic wrap.

11. In the dark room the wrapped membrane was placed, protein side up, in a film cassette.
12. A sheet of auto-radiography film was placed on top of the membrane and the cassette was closed.
13. The film was exposed; for the optimal detection of phospho-AMPK the film was exposed overnight. The optimal detection of non-phosphorylated AMPK required 2 to 3 minutes of exposure. The optimal detection of both cytoplasmic and nuclear NF- B also required 2 to 3 minutes of exposure.
14. Protein band intensity was quantified using the Kodak 1D Image Analysis Software v3.6.

2.3.5 Amido black staining

Amido black staining was performed after each ECL detection experiment for the cytoplasmic and nuclear NF- B of U1 cells. This was to verify whether the observed difference in the cytoplasmic and nuclear concentrations of NF- B, between metformin and AICAR treated cells and the control cells, was due to the effects of AICAR and metformin, and not due to unequal amounts of protein loaded in the wells. Amido black is a non-reversible stain that produces dark bands on a light background.

Required reagents:

Amido black stain (appendix II),
destain solution (appendix II),
100 % methanol,
ultra-pure water.

1. A dry blot was first re-wetted in 100 % methanol for 15 seconds.
2. A tray was filled with enough stain to cover the blot and the blot was placed in the stain and agitated for 10 minutes.
3. The blot was removed and rinsed briefly in ultra-pure water.
4. The blot was then placed in destain solution and agitated for 5 to 10 minutes to remove excess stain.

2.3.6 Statistical analysis

The Wilcoxon matched pairs test, using Statview, was used for all statistical calculations. The difference between means with a p-value of ≤ 0.05 was considered to be statistically significant. Data in histograms is expressed as mean \pm SD.

CHAPTER 3

RESULTS

3.1 3T3-L1 Results

3.1.1 Optimization of AICAR and metformin concentration for adipogenesis

3T3-L1 were cultured in the presence of three different concentrations of AICAR 0.5 mM, 0.75 mM, and 1 mM; and three different concentrations of metformin 2 mM, 3 mM, and 4 mM. AICAR at the concentration of 1 mM had the highest inhibition of adipogenesis.

Therefore, 1 mM AICAR was used as the adipogenesis inhibition control (positive control) in all the subsequent experiments.

Among the three concentrations of metformin used; 2 mM, 3 mM, and 4 mM; a significant inhibition of adipogenesis was observed only with 4 mM. Therefore, we decided to start all the future experiments with 2 mM of metformin and increase the concentration two fold up to 16 mM i.e. 2 mM, 4 mM, 8 mM, and 16 mM.

3.1.2 Comparing 3T3-L1 lipid content at confluence (day 0) and at the end of adipogenesis (day 8) and after treatment with AICAR and metformin

The amount of triglyceride in 3T3-L1 on day 0 and day 8 were compared by comparing the spectrophotometric readings of Oil red O on day 0 and day 8. The results showed that the induction of adipogenesis resulted in a 3 fold increase in intracellular lipid content of 3T3-L1 (figure 3.1).

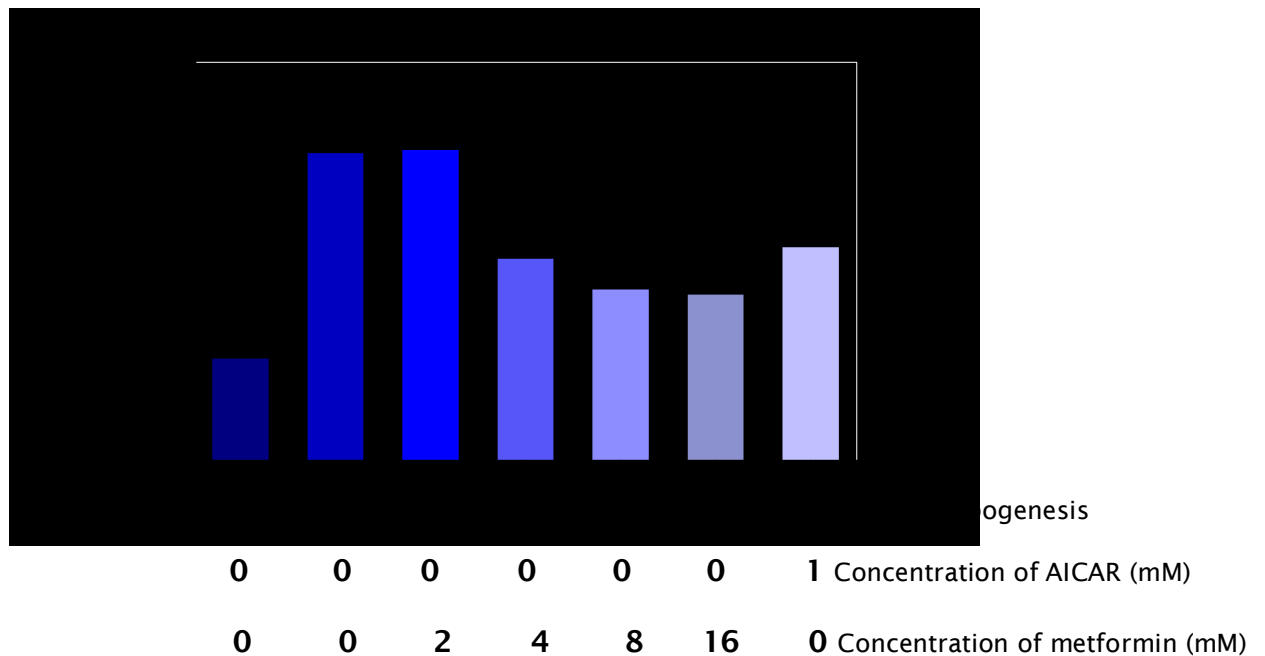


*Figure 3.1: the induction of adipogenesis increased the intracellular lipid content 3-fold from base line after eight days of adipogenesis, * $p < 0.05$ day 0 vs day 8. AICAR and metformin significantly inhibit intracellular lipid accumulation in 3T3-L1, * $p < 0.05$ vs 0 mM after 8 days of adipogenesis. Data expressed as mean \pm SD, $n = 6$.*

Metformin at a concentration of 2 mM did not have any effect on the inhibition of triglyceride accumulation in 3T3-L1. However, significant inhibition of intracellular lipid was observed with 4, 8, and 16 mM of metformin (figure 3.1). It was also observed that the inhibition of lipid accumulation reached its peak at 8 mM (figure 3.1). Cells cultured with 8 mM metformin had 45 % less lipid than the untreated cells.

Cells treated with 1 mM AICAR also had significantly less intracellular lipid than the control cells. AICAR treated cells had approximately 35 % less lipid than the controls (figure 3.1).

3.1.3 Comparing protein concentrations of 3T3-L1 treated with metformin or AICAR and the control cells.

Table 3.1: concentrations (in $\mu\text{g}/\text{mL}$) of protein extracts from 3T3-L1 cells.

	Negative control	Metformin 16 mM	AICAR 1mM
Experiment 1	259.4	540.8	551.5
Experiment 2	473.5	582.6	329.0
Experiment 3	1610.3	1461.9	1239.4
Experiment 4	1416.7	963.6	1222.1
Experiment 5	1529.9	1236.6	1175.6
Mean	1058.0	957.1	903.5
Standard deviation	639.5	402.0	430.8

There was no statistically significant difference between the protein concentrations from the control cultures and the protein concentration

from cells treated with metformin ($p = 0.2367$) (table 3.1). There was also no statistically significant difference between the protein concentration from the control cultures and the protein concentration from cells treated with AICAR ($p = 0.1282$) (table 3.1). The protein concentrations from metformin treated cells and AICAR treated cells, as well, did not show statistically significant difference ($p = 0.6858$) (table 3.1).

3.1.4 Western blotting for phospho-AMPK

After 8 days of adipogenesis, the results of the Western blotting experiment of cells treated with 16 mM metformin and cells treated with 1 mM AICAR compared to controls suggested that there may be a relationship between the activation of AMPK and the accumulation of lipid in 3T3-L1. As shown in figure 3.2, there was a marked increase in the phosphorylation of AMPK in the presence of AICAR, and metformin, while the amount of phosphorylation in untreated cells remained comparable to phosphorylation on day 0.

The net intensity of bands of AMPK phosphorylated at threonine 172 (AMPK-Thr172) on day 8 for metformin, AICAR, and control cells were measured after each Western blotting experiment, using the Kodak 1D Image Analysis Software v3.6, and the results were plotted. AMPK

phosphorylation by metformin and AICAR was 4 to 5 fold higher than the phosphorylation of the enzyme in the control group (figure 3.3).

1. 2. 3. 4.



Figure 3.2: Western blotting of total protein from 3T3-L1 on day 0 (lane 1), from control 3T3-L1 cells on day 8 of adipogenesis (lane 2), and from 3T3-L1 treated with AICAR and metformin (lane 3 and 4 respectively) on day 8. This blot is a representative of 5 different experiments. Polyclonal antibody specific to phospho-AMPK was used.

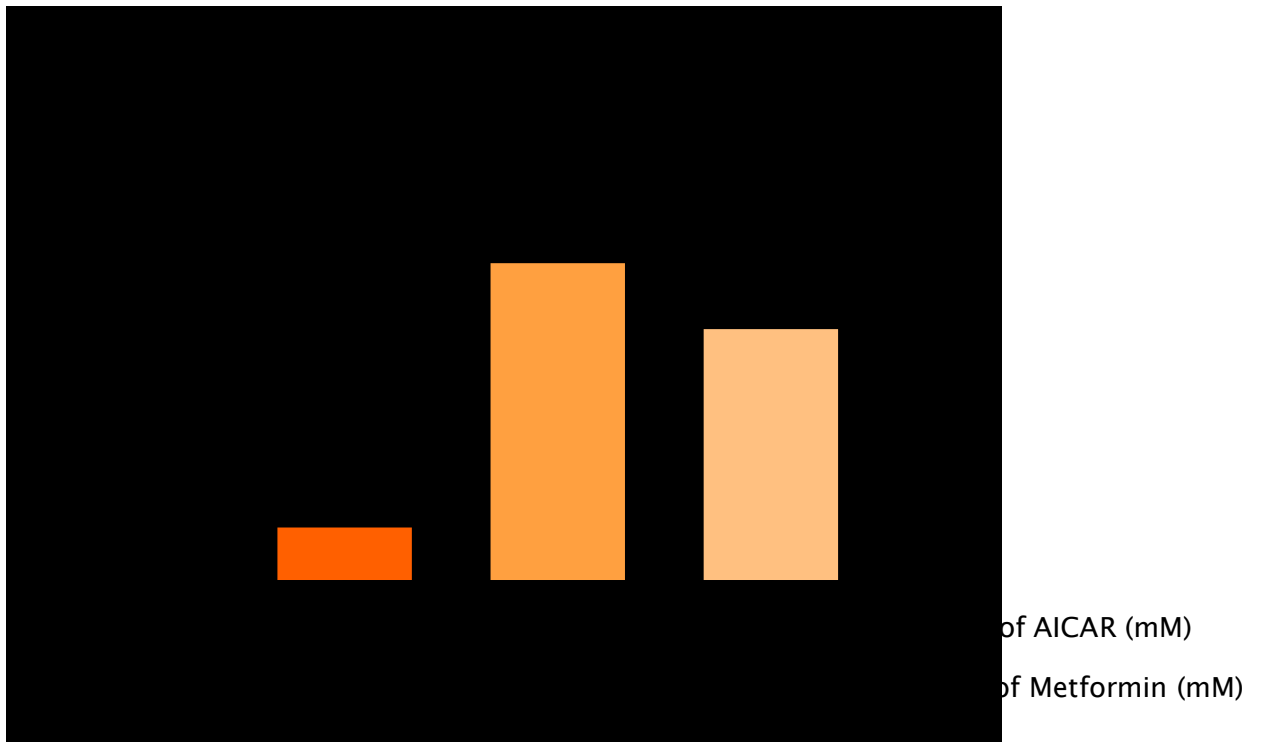


*Figure 3.3: Comparison of the level of AMPK phosphorylation on day 8 of adipogenesis, for metformin and AICAR treated cells versus controls, using the Kodak 1D Image Analysis Software v3.6. Data expressed as means \pm SD from 5 experiments, * $p < 0.05$ versus control cells.*

3.2 U1 results

3.2.1 Optimization of AICAR and metformin concentration for inhibition of HIV-1 replication in U1 cells

There was no viable U1 cell after 48 hours of tissue culture with 1 mM AICAR (figure 3.4). A 50 % loss of viability was observed with U1 cells cultured with 0.5 mM AICAR (figure 3.4). 0.4 mM AICAR showed a very strong inhibition of HIV-1 replication (figure 3.5) and this concentration did not seem to be toxic to U1 cells (figure 3.4). For metformin the strongest inhibition of HIV-1 replication was observed with 16 mM (figure 3.5) and the viability of cells cultured with this concentration was comparable to that of the control culture (figure 3.4). The optimization experiment was carried out only once. The p24 concentrations obtained in this experiment were much higher than those obtained in the subsequent experiments. This could be attributed to differences in the cell passage number between experiments.

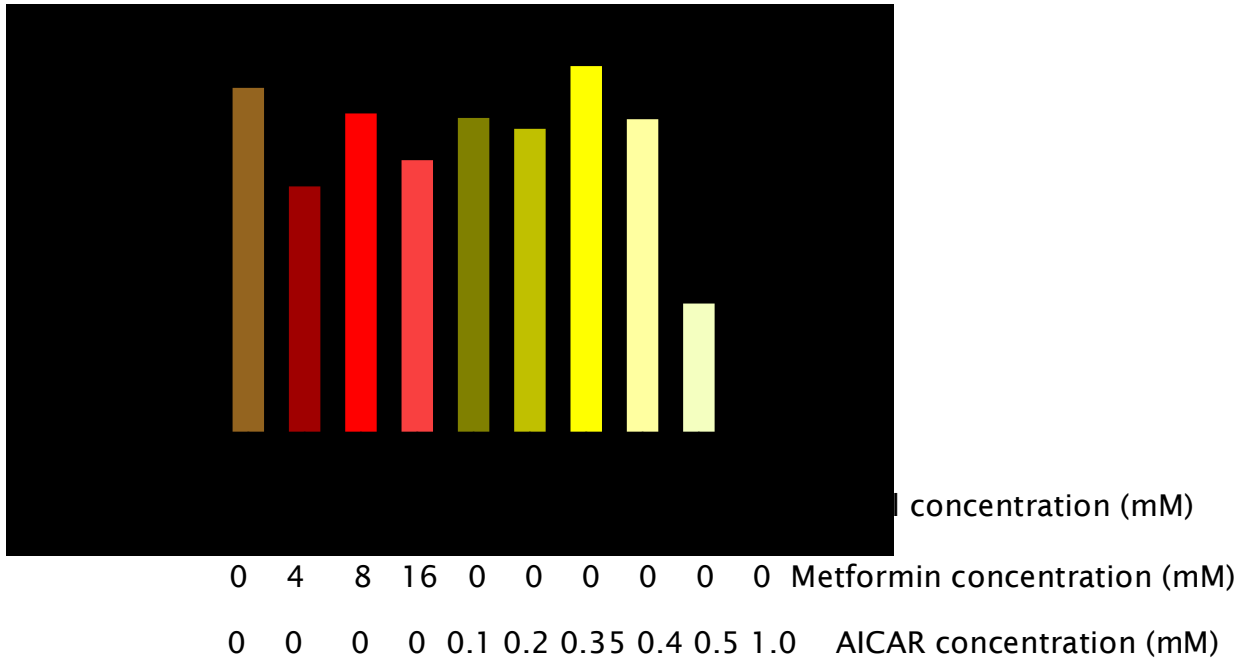


Figure 3.4: U1 Cell count after culturing the cells with metformin and AICAR and activating HIV-1 replication with 60 mM NaCl.

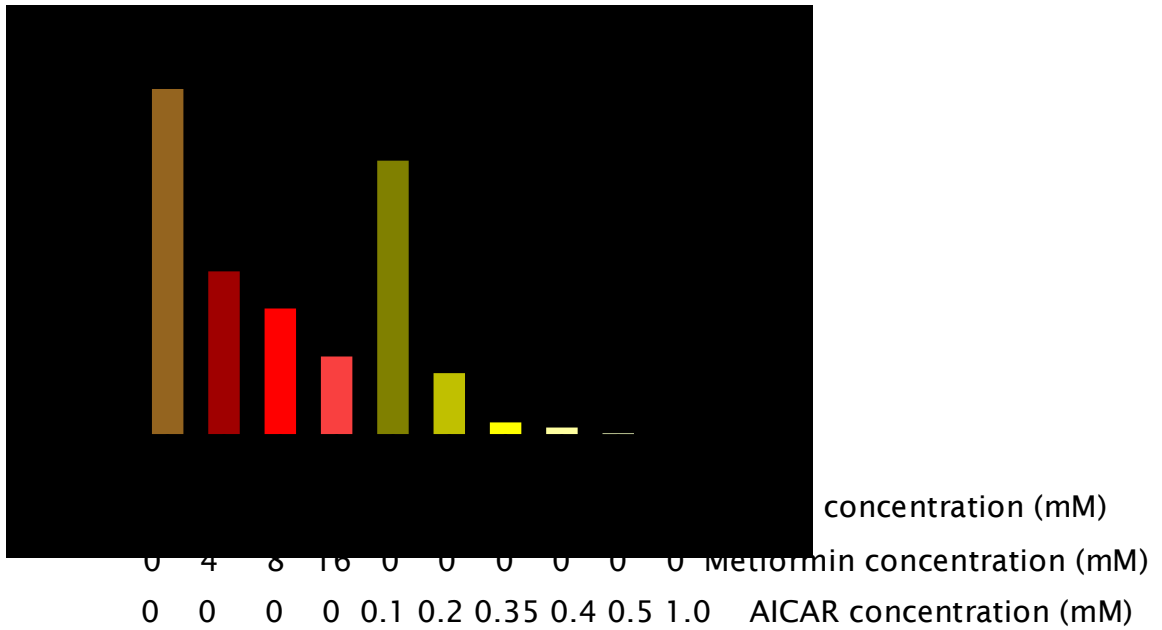
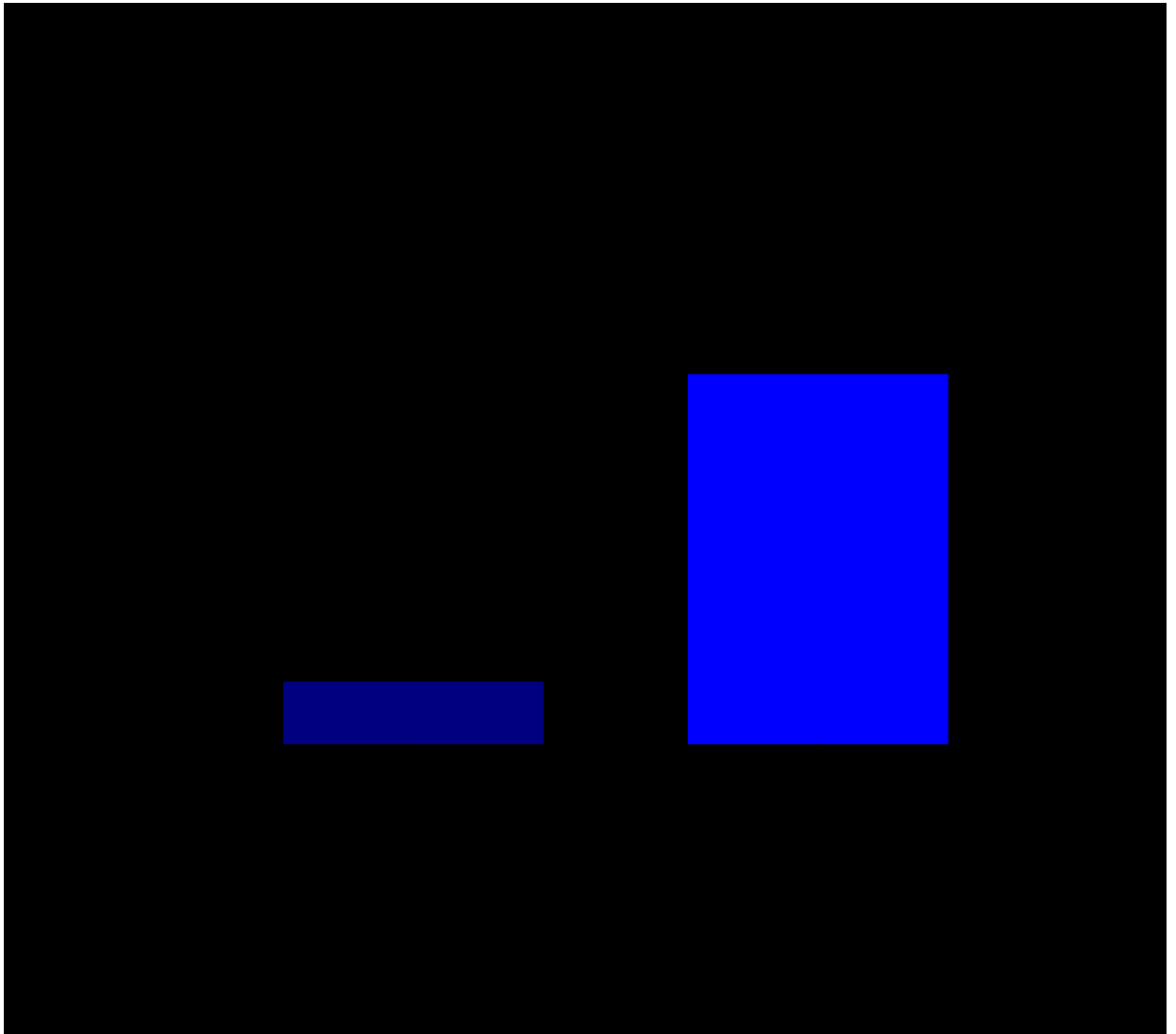


Figure 3.5. Determination of metformin and AICAR concentrations that had the strongest inhibition of HIV-1 replication in U1 cells.

3.2.2 NaCl activates HIV-1 replication in U1 cells

The ability of 60 mM NaCl to induce HIV-1 replication in U1 cells was measured by comparing the rate of HIV-1 replication, after 2 days of tissue culture, between U1 cells treated with 60 mM NaCl and untreated U1 cells. The ELISA results indicated that 60 mM NaCl treated cells had an increase in HIV-1 replication of approximately 5 folds from baseline (figure 3.6).

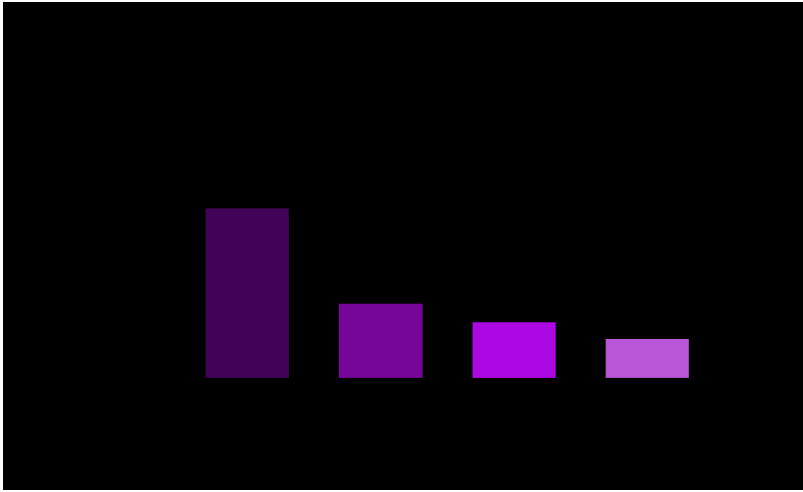


*Figure 3.6. U1 cells treated with 60 mM of NaCl have an increase in HIV-1 replication of about 5 fold, compared to untreated cells. Data expressed as mean \pm SD from 7 experiments; * $p < 0.05$ versus untreated cells.*

3.2.3 AICAR and metformin inhibit HIV-1 replication in U1 cells

The results of p24 ELISA, after 48 hours of incubating the cells in medium containing AICAR or metformin, showed a marked inhibition of HIV-1 replication by both molecules. The concentration of p24 decreased with increasing concentrations of either AICAR or metformin (figures 3.7 A and B). The means of p24 values as percentage of the control culture (cells cultured with 60 mM NaCl only) are also shown in table 3.2 for metformin, and table 3.3 for AICAR.

A.



B.

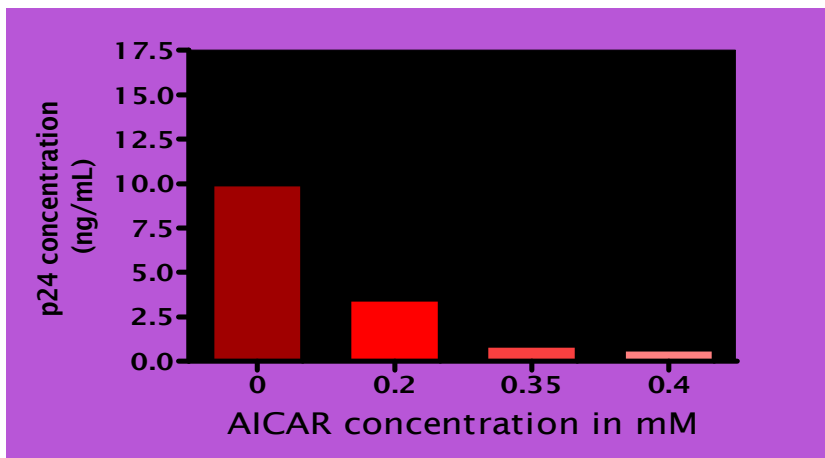


Figure 3.7: (A) Plot of P24 concentrations after 48 hours of HIV-1 replication in U1 cells cultured with different concentrations of metformin. Data expressed as mean \pm SD from 8 experiments; * $p < 0.05$ versus 0 mM metformin. (B) P24 concentrations after 48 hours of HIV-1 replication in U1 cells cultured with different concentrations of AICAR. Data expressed as mean \pm SD from 9 experiments; * $p < 0.05$ versus 0 mM AICAR.

Table 3.2: Mean p24 values as percentage of controls, after 2 days of tissue culture, for U1 cells treated with metformin.

	Control cells	Metformin 4mM	Metformin 8mM	Metformin 16mM
Mean	100.00	35.462	27.384	28.411
Standard deviation	0.00	17.065	8.718	9.961

P-value < 0.05, n = 8.

Table 3.3: Mean p24 values as percentage of controls, after 2 days of tissue culture, for U1 cells treated with AICAR.

	Control cells	AICAR 0.2mM	AICAR 0.35mM	AICAR 0.40mM
Mean	100.0	61.7	16.7	14.1
Standard deviation	0.0	32.8	8.2	10.5

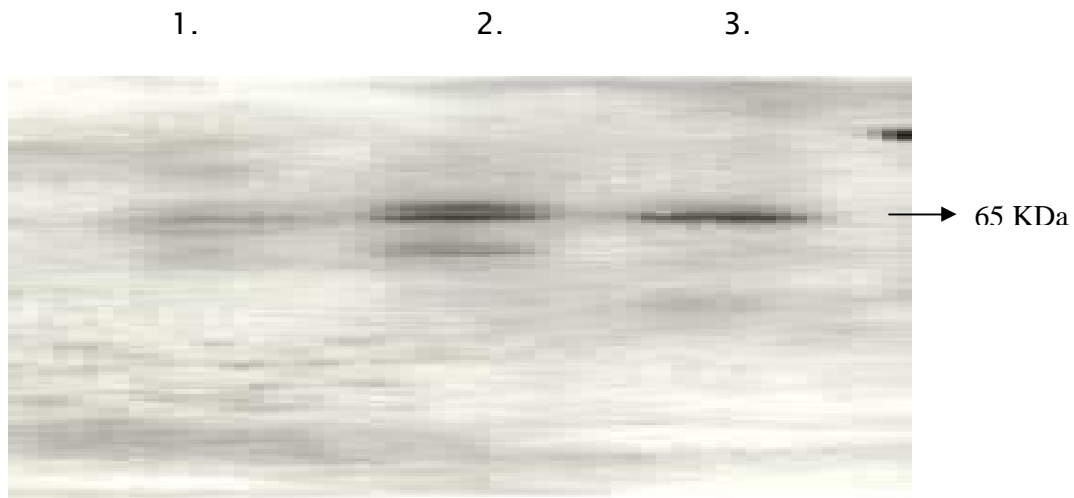
P-value < 0.05, n = 9.

3.2.4 AICAR and Metformin inhibit NF- κ B translocation from the cytoplasm to the nucleus

To determine whether the inhibition of HIV-1 replication by AICAR and metformin was due to the inhibition of NF- κ B translocation from the cytoplasm to the nucleus, Western blotting of the cytoplasmic and nuclear extracts of U1 cells was performed. AICAR treated cells had the highest accumulation of NF- κ B in their cytoplasm, followed by metformin treated cells, while the lowest amount of cytoplasmic NF- κ B was observed in the control cells (figure 3.8 A). This experiment was repeated 3 times.

In the nucleus the inverse of the cytoplasmic Western blots was observed. Control cells had the highest amount of NF- κ B in their nucleus followed by metformin treated cells and AICAR treated cells had the lowest amount of NF- κ B (Figure 3.8 B).

A.



B.

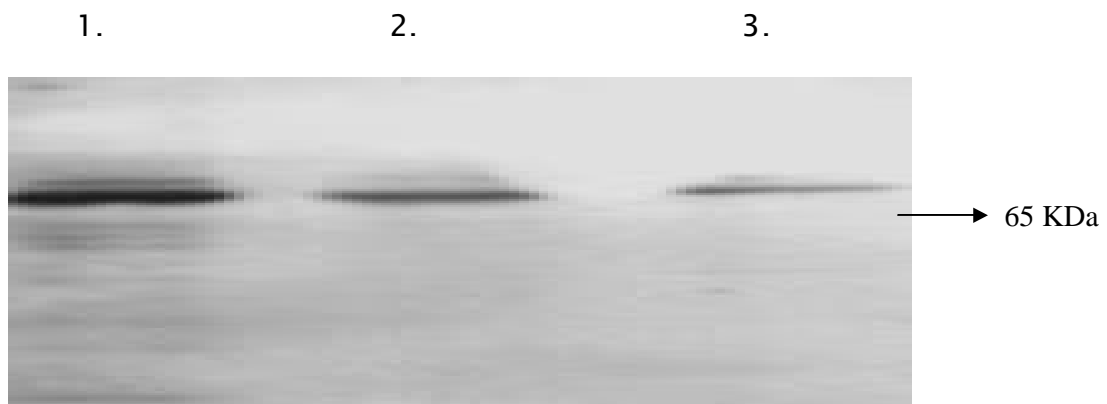
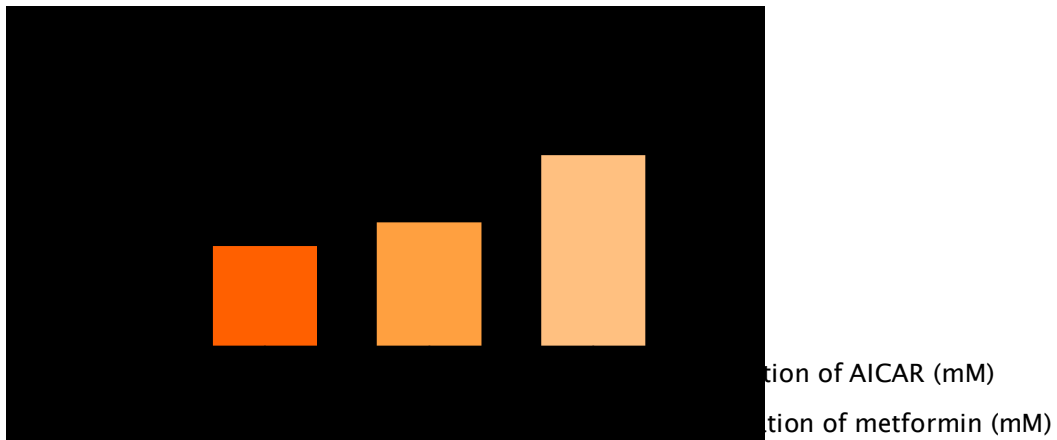


Figure 3.8: (A) Western blotting of the cytoplasmic extracts of U1 cells with anti-NF- κ B antibody: control cells, lane 1, metformin treated cells, lane 2; AICAR treated cells, lane 3. This is representative of 3 Western blots. 4 μ g of protein were loaded in each well (B) Western blotting of the nuclear extracts of U1 cells with anti-NF- κ B antibody: control cells, lane 1, metformin treated cells, lane 2, and AICAR treated cells, lane 3. This blot is representative of 5 Western blots. 4 μ g of protein were loaded in each well.

The net intensity of the NF- κ B bands on day 2 for metformin, AICAR, and control cells were measured after each Western blotting experiment, using the Kodak 1D Image Analysis Software v3.6 and the results were plotted. Although there was no statistical significance, the level of NF- κ B in the cytoplasm of cells treated with metformin and AICAR was higher than the level of NF- κ B in the cytoplasm of the control culture (figure 3.9 A). The graph of the nuclear NF- κ B net intensities showed a significantly higher accumulation of the nuclear factor in the nucleus of the controls compared to metformin and AICAR treated cells (figure 3.9 B).

A.



B.

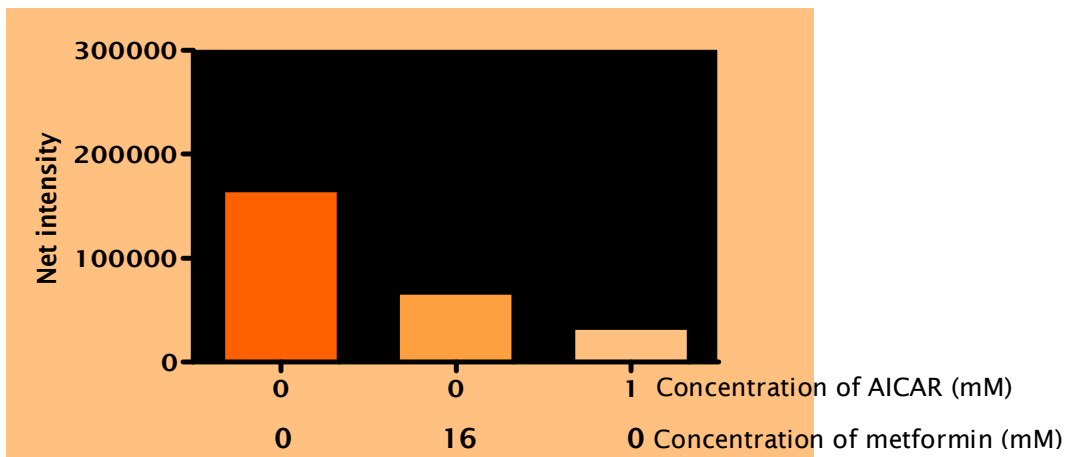


Figure 3.9: (A) Comparison of the cytoplasmic level of NF-κB in metformin and AICAR treated cultures and control cells. Data is expressed as mean \pm SD from 3 experiments. (B) Comparison of the nuclear level of NF-κB in metformin and AICAR treated cells and control cells. Data is expressed as mean \pm SD from 5 experiments; * $p < 0.05$ versus controls.

The membranes on which the cytoplasmic and the nuclear proteins were transferred were stained with amido black (figure 3.10 and 3.11). The results showed that an equivalent amount of protein was loaded in all but well 2 (lane 2) of figure 3.11. However, it is unlikely that this has interfered with the outcome of the experiment because the control culture (lane 1, figure 3.11) still had more nuclear NF- B than metformin treated culture (lane 2, figure 3.11), see figure 3.8 (B) and 3.9 (B).



Figure 3.10: Amido black staining of the membrane used for Western blotting of the cytoplasmic extracts of U1 cells. Lane 1 and 5, molecular weight markers; lane 2, control cells; lane 3, metformin treated cells; lane 4, AICAR treated cells.



Figure 3.11: Amido black staining of the membrane used for Western blotting of the nuclear extracts of U1 cells. Lane 1, control cells; lane 2, metformin treated cells; lane 3, AICAR treated cells, lane 4, molecular weight markers.

3.2.5 AMPK expression in U1 cells

Western blotting with antibody specific to the α -subunit of AMPK was performed to investigate whether AMPK was expressed in U1 cells. The results showed that the kinase is expressed in this cell line (figure 3.12).

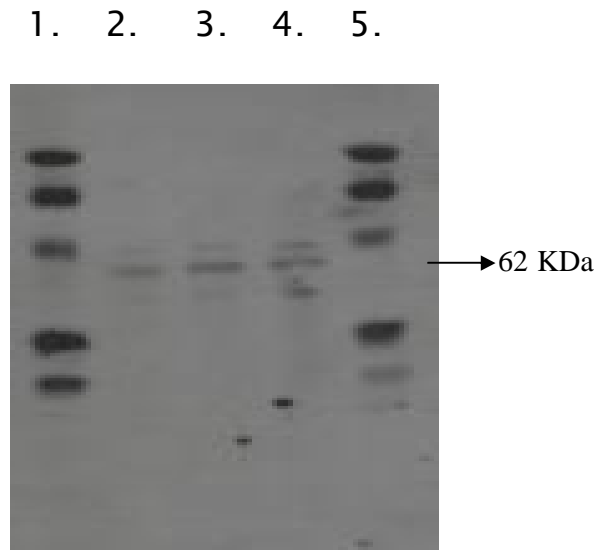
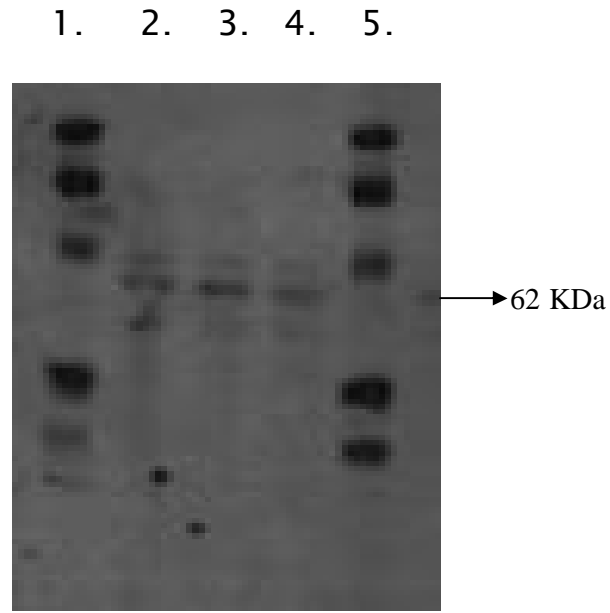


Figure 3.12: Western blotting of U1 cells total protein with antibody specific to the α -subunit of AMPK. Lanes 1 and 5, molecular weight markers, lane 2 control cells, lane 3, metformin treated cells, and lane 4, AICAR treated cells. This experiment was repeated twice, top and bottom membrane.

3.2.6 AICAR and metformin do not phosphorylate AMPK at threonine 172 in U1 cells

To show that metformin and AICAR inhibited the translocation of NF- κ B via activation of AMPK, Western blotting with antibody specific to AMPK phosphorylated at Thr-172 was done with the cytoplasmic extracts of U1 cells. The antibody was unable to detect any phosphorylation of AMPK at Thr-172 after 48 hours of treatment with AICAR or metformin. The experimental time was reduced to 45 minutes to allow for the possibility that AMPK may have been dephosphorylated after 48 hours. After 45 minutes no phosphorylation of AMPK was observed. All these Western blots were repeated three times.

We also verified whether the inability to observe the phosphorylation of AMPK was caused by the Western blotting method used. This was done by performing the Western blotting of phospho-AMPK in U1 cells (cultured with AICAR and metformin for 45 minutes) together with the western blotting for phospho-AMPK in 3T3-L1 (figure 3.13). The result showed that the inability to observe the phosphorylation of AMPK in U1 cells was not due to the Western blotting method used, because phospho-AMPK could be detected in 3T3-L1 using the same method.

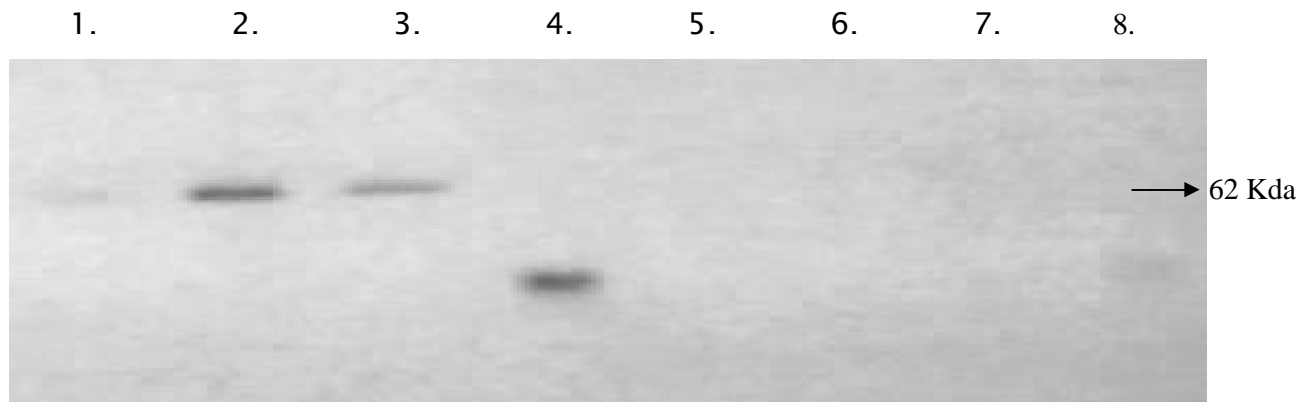


Figure 3.13: AMPK is phosphorylated in 3T3-L1 but not in U1 cells. Lane 1, 3T3-L1 cultured without AICAR and metformin (controls or untreated cells); lane 2, 3T3-L1 cultured with AICAR, lane 3, 3T3-L1 cultured with metformin; lane 4 and 8, molecular weight markers; lane 5, U1 cells cultured with 60 mM NaCl only (controls); lane 6, U1 cells cultured with metformin; lane 7, U1 cells cultured with AICAR.

CHAPTER 4
DISCUSSION

4.1 Metformin inhibits adipogenesis in 3T3-L1

The present and a previous study [25] have both shown that AICAR inhibits adipogenesis in 3T3-L1 cells. This occurs by down-regulation of expression of the lipogenic enzymes ACC and FAS and of the adipogenic transcription factors peroxisome proliferator-activated receptor (PPAR) γ and CCAAT/enhancer binding protein (C/EBP) α [25].

The present study is the first to demonstrate that the inhibition of intracellular lipid accumulation in 3T3-L1 cells by AICAR or metformin is paralleled by increased phosphorylation of AMPK at residue Thr-172 of the catalytic α -subunit. The phosphorylation of AMPK at this site is essential for its function and activated AMPK is known to inhibit the lipogenic enzyme ACC by phosphorylation [83, 84].

This study demonstrates that culturing preadipocytes in the presence of metformin results in increased phosphorylation of AMPK at Thr-172 and accumulation of significantly less lipid than in non-treated cells. These data suggest that in 3T3-L1 cells undergoing adipogenesis, metformin activates AMPK, which in turn leads to the inhibition of intracellular lipid accumulation. This hypothesis is supported by an earlier study [9], showing that metformin treatment of rodent primary hepatocytes leads to AMPK activation, via increased phosphorylation at Thr-172, and inhibition of ACC activity. The inhibitory effect of metformin and AICAR on ACC activity was attenuated by an inhibitor of AMPK, compound C

[9]. Metformin inhibited gene expression of lipogenic enzymes FAS, and the lipogenic transcription factor, sterol regulatory enhancer binding protein (SREBP-1) [9]. These effects on gene expression were observed in both treated primary hepatocytes and in liver tissue isolated from rats treated with metformin [9]. Another study has also shown that treatment of the human hepatocyte cell line, HepG2, with metformin results in reduced intra-cellular lipid accumulation [38].

The present study suggests that metformin is able to reduce intra-cellular lipid accumulation during adipogenesis by the activation of AMPK. Other studies show that this effect of AMPK may be due to the inhibition of lipogenic enzymes and the down regulation of transcription factors involved in lipogenesis [25] [1, 6]. Thus, the ability of metformin to limit weight gain in human subjects may be partially mediated by metformin's actions on adipogenesis but it is probable that metformin may also inhibit lipid accumulation in mature adipocytes. However, this study does not show whether the activation of AMPK in adipose tissue was directly involved in the inhibition of lipid accumulation. There is still a possibility that the observed AMPK activation is simply a result of metformin altered cellular metabolism and has no involvement in the inhibition of lipid accumulation. Therefore, a study with inhibitors of AMPK, such as compound C [9] or AMPK specific small interfering RNAs (siRNAs), may be required to

confirm whether or not AMPK is involved in the metformin induced inhibition of intracellular lipid accumulation.

It is also important to note that, although intracellular lipid accumulation is a key feature of adipogenesis, adipogenesis is a process that also involves the expression of genes such as PPAR γ , C/EBP α and C/EBP β [45]. Here we have simply shown that metformin inhibits one aspect of adipogenesis i.e. intra-cellular lipid accumulation and this inhibition is likely to be mediated by AMPK. However, it remains to be shown whether the activation of AMPK by metformin also involves the inhibition of the expression of pro-adipogenesis genes mentioned above.

We are aware that the concentrations of metformin used to inhibit intracellular lipid accumulation by other researchers, such as Zhou *et al.* who used 0-2000 μ M [9] were lower than the ones used in our study, 2000-16000 μ M. This difference may be attributed to the different tissues used in these studies. Thus, Zhou and co-workers worked on hepatocytes while our study was based on adipocytes.

The possibility that the observed inhibition of intracellular lipid accumulation by metformin is due to toxicity to adipocytes cannot be ignored. Metformin has been reported to be toxic to the mitochondria [21]. Nevertheless, we have two main reasons to believe that the observed inhibition of lipid accumulation was not due to the toxicity of metformin to the cells. The first is that 3T3-L1 are adherent cells i.e.

they grow by attaching to the surface of the flask in which they are cultured. When these cells lose their viability they detach from the surface. Because the experiment was performed over 8 days, with the medium being changed every two days, it would have been very easy to observe cell detachment. Secondly, the amount of protein extracted from the cells on day 8 does not suggest that metformin had a deleterious effect on cell growth. If metformin had killed the cells in culture, the amount of proteins extracted from the remaining cells would have been much smaller than the amount of protein extracted from untreated cells and AICAR treated cells. However, this was not the case (see table 3.1).

It should also be mentioned that the finding that mannitol can activate AMPK by phosphorylation [34] raises some concerns as the cell lysis buffer used in the study contained mannitol (appendix II). However, if the observed phosphorylation of AMPK was caused by a reagent in the lysis buffer rather than by metformin or AICAR, it is clear that we would have observed a similar phosphorylation of AMPK in metformin, AICAR, and the control cells. However, as shown in figures 3.2 and 3.3, there was a clear difference in AMPK phosphorylation between the three groups.

This study is the first to demonstrate a possible mechanism for the weight loss associated with the use of metformin in type 2 diabetic patients. The data presented in this report is complemented by another

study that shows the effects of AMPK activation by metformin on downstream enzymes, such as acetyl-CoA carboxylase and fatty-acid synthase, enzymes involved in fatty acid metabolism. As shown by Habinowsky and Witters [25] AMPK activation in 3T3-L1 with AICAR results in the inhibition of downstream enzymes involved in fatty acid biosynthesis.

Finally, the use of AICAR as a positive control in this experiment is not ideal, for AICAR has been reported to target other intracellular enzymes, besides AMPK [25]. Nevertheless, AICAR is the most well known activator of AMPK and has been used in many studies of the AMPK signaling system [9, 25, 38]. It should also be mentioned that it would have been ideal to use a house keeping gene such as β -actin in our Western blotting experiments. However, it is also noted that similar studies [9] to ours have also not used house keeping genes to control for protein loading on Western blots.

4.2 Metformin and AICAR inhibit HIV-1 replication in U1 cells

In this report we have also been able to show that metformin and AICAR have inhibitory properties on HIV-1 replication in U1 cells. This inhibition is dose dependent i.e. increases as the concentration of these two molecules increases. A possible mechanism of inhibition of HIV-1

replication by AICAR and metformin is the inhibition of NF- κ B translocation to the nucleus. This is shown by the increased accumulation of NF- κ B in the cytoplasm of AICAR and metformin treated cells compared to the control cells and the reduced amount of this factor in the nuclei of these cells compared to the control cells. The absence of NF- κ B in the nucleus results in the inhibition of HIV-1 gene transcription. However, it is still unclear which enzyme mediates the inhibition of NF- κ B translocation to the nucleus. AICAR and metformin are well known activators of AMPK, and the enzyme is expressed in U1 cells, as shown in figure 3.12. However, we failed to observe any phosphorylation of the kinase by both drugs.

Our study therefore suggests that in monocytes, both AICAR and metformin do not activate AMPK or they do via a mechanism other than phosphorylation at threonine 172 of the α -subunit. Under the belief that AICAR and metformin did activate AMPK by phosphorylation and that this phosphorylation might have lasted for only a short period of time, we set up the same experiment but for a much shorter duration i.e. 45 minutes instead of 48 hours. However, we still did not manage to observe any phosphorylation of AMPK in these cells by either molecule. It may also be argued that AMPK phosphorylation was complete in 5 minutes that is why we couldn't detect any phosphorylation after 45 minutes. A counter argument to this, however, is that in 3T3-L1 the enzyme remains phosphorylated even 48 hours after activation. It is

also unlikely that a phosphorylation that lasted only few minutes will have such a strong effect on HIV replication after 48 hours.

The fact that phospho-AMPK couldn't be detected does not mean that AMPK phosphorylation may not play a role in the inhibition of NF- κ B translocation to the nucleus, in U1 cells. The best way to confirm the involvement of AMPK in the inhibitory pathway of NF- κ B translocation to the nucleus is by either using one of the pharmacological inhibitors of AMPK e.g. compound C [9] or adenine 9- β -D-arabinofuranosine [75] or siRNAs, which are more specific inhibitors of the enzyme. It is noteworthy that a study by Guigas *et al.* [85] showed that AICAR and metformin could inhibit the glucose induced translocation of glucokinase from the nucleus to the cytosol via an AMPK independent mechanism. Guigas *et al.* proposed the decrease in intracellular ATP concentrations to be responsible for this inhibition [85].

It is possible that the inhibition of HIV-1 replication by AICAR and metformin was simply due to the toxic effects of these drugs to U1 cells. However, our results (figure 3.4) show that U1 cells cultured with AICAR and metformin, at the concentrations used in the study, had comparable viability to U1 cells cultured without AICAR or metformin. We should also mention that we obtained high standard deviations between different experiments in this study, which is one of the set backs of the study. We believe this is most probably due to the difference in the cell passage number for different experiments.

Nevertheless, the difference in the p24 concentrations between metformin or AICAR treated cells when compared to the control group was statistically significant. It can also be argued that the difference in cytoplasmic and nuclear NF- κ B was simply due to unequal amount of proteins loaded in each well of the gel. However, it should be noted that our Western blotting experiments were repeated at least 3 times to minimize such a possibility. Also the Bradford method was used to determine the protein concentrations, we believe if there is no error in the calculations it is possible to load the same amount of protein in different wells of the gel.

NF- κ B plays an important role in the initiation of HIV-1 gene transcription [7, 63, 73]. HIV-1 LTR is made of two highly conserved copies of the κ B elements [63] which are crucial for RNA transcription of the integrated provirus. However, there are some major differences in the HIV-1 and HIV-2 genome [56, 86]. These two viruses rely on different enhancers to control their gene transcription. Hannibal and colleagues showed that TNF- α activation of HIV-1, which is mediated by NF- κ B binding to the κ B element, is many fold higher than the activation of HIV-2 [86]. Most importantly, Hannibal and his group reported that while HIV-1 gene transcription relies solely on NF- κ B, there are other factors that also regulate gene transcription in HIV-2 [86]. This suggests that metformin and AICAR may not have a significant inhibitory activity against HIV-2.

Our results suggest the possibility of using AICAR and metformin to treat HIV-1 infection. This by preventing latently infected cells becoming sites of HIV-1 replication, via inhibition of the transcription factor needed for HIV-1 gene transcription. Since these compounds modify the host's response rather than directly target the virus, they may also be less vulnerable to the high rate of mutations taking place in the viral genome.

Lastly, not only is metformin or AICAR relatively cheap when compared to existing antiretrovirals, they are also less toxic. For example the overall incidence of lactic acidosis associated with metformin is about 0.05 cases per 1000 patients per year [22], and AICAR is safely used to treat ischemic heart disease [28, 29]. Furthermore, metformin has been successfully used to treat lipodystrophy in HIV positive patients [87] with no negative side effects. However, this study did not look at the viral loads of these patients as they were also being treated with anti-retrovirals, which could mask the effects of metformin. The toxicity of antiretrovirals has already been discussed in section 1.7.10.

In conclusion, metformin and AICAR reduce intracellular lipid accumulation in the 3T3-L1 cells, most probably by activation of AMPK. Furthermore, both these agents are able to inhibit HIV-1 replication in U1 cells, and this may occur via down regulation of nuclear NF- κ B levels. The involvement of AMPK in this process is not certain.

APPENDIX

APPENDIX I

REAGENTS

Dexamethasone, 3-isobutyl-1-methylxanthine (IBMX), AICAR and metformin were obtained from Sigma-Aldrich (St. Louis, Missouri, USA). Insulin was supplied by Novo Nordisk (Copenhagen, Denmark). The Dulbecco modified Eagle's medium (DMEM), foetal calf serum (FCS), penicillin, streptomycin, trypsin, sodium pyruvate, and L-glutamine were purchased from Gibco-Invitrogen, (Carlsbad, California, USA). RPMI 1640 came from Biowhittaker, Walkersville, U.S.A. The phospho-AMPK (Thr172) and the pan α AMPK antibodies were obtained from Cell Signaling Technology, Inc. (Beverly, Massachusetts, USA). Goat anti-rabbit-HRP antibody, used as secondary antibody against phospho-AMPK, was obtained from DakoCytomation (Glostrup, Denmark). Rabbit anti-sheep-HRP antibody, used as secondary antibody against pan α AMPK antibody, also came from DakoCytomation, (Glostrup, Denmark). The antibody specific to NF- κ B was supplied by EMD Biosciences, Inc., an affiliate of Merck KGaA (Darmstadt, Germany). The goat anti-rabbit-HRP antibody used as secondary antibody against NF- κ B came from DakoCytomation (Glostrup, Denmark). The enhanced chemiluminescent (ECL) reagents, Hybond-P PVDF membrane, ECL[™] detection reagents and Hyperfilm ECL, were provided by Amersham Biosciences UK Limited

(Little Chalfont, Buckinghamshire, UK). The Oil red O dye came from Sigma-Aldrich (St. Louis, Missouri, USA). Low passage number 3T3-L1 cell line, pre-adipocytes that can be transformed into adipocytes, were obtained from the European Collection of Cell Cultures (number 86052701). The U1 cell line, HIV-1 chronically infected monocytes, was obtained from the NIH AIDS Research and Reference Reagent Program, NIAID. Trans-blot filter papers were from Biorad (Hercules, California, USA). Molecular weight markers Kaleidoscope prestained standards were from Biorad (Hercules California). NucBuster used to extract total nuclear and cytoplasmic protein was from EMD Biosciences, Inc., an affiliate of Merck KGaA (Darmstadt, Germany). The p24 assay kit came from Dupont (DuPont, Boston, MA). Trypan blue was purchased from Sigma-Aldrich (St. Louis, Missouri, USA).

APPENDIX II

BUFFERS AND SOLUTIONS FOR PROTEIN ELECTROPHORESIS AND WESTERN BLOTTING

Composition of DMEM maintenance medium:

100mL of maintenance medium:

DMEM	1.35 g
Sodium bicarbonate	0.37 g
Fetal calf serum	10.0 mL
Penicillin	100 U
Streptomycin	100 U
Sodium pyruvate	1 mM
L-glutamine	2 mM

Stacking gel buffer (pH 6.8):

0.5M tris-HCl:

Tris	6 g
Water	40 mL

Take the pH to 6.8 with hydrochloric acid (2 M). Make up to 100 mL with water.

Resolving gel buffer:

Tris	36.3 g
HCl (2M)	24 mL
Water	100 mL

Stock reservoir buffer (pH 8.3):

Tris	3.03 g
Glycine	14.4 g
SDS	1 g
Water	1 L

Ammonium persulphate solution (3%):

300 mg of ammonium persulphate in 10 mL of water.

Note that the ammonium persulphate must be freshly made before use.

Stock acrylamide bis solution:

Acrylamide	30 g
Bisacrylamide	0.4 g
Water	100 mL

Filter with a Whatman filter paper, cover with foil and store in the fridge.

Sodium dodecyl sulphate solution (SDS) (10%):

Sodium dodecyl sulphate	1 g
Water	10 mL

SDS gel preparation:

Resolving gel:

Acrylamide/Bis	8.3 mL
Resolving buffer	2.5 mL
10% SDS	0.2 mL
1.5% ammonium persulfate	1 mL
Water	9.6 mL
TEMED	10 μ L

Note: the gel should be de-aerated prior to addition of ammonium persulfate.

Stacking gel:

Acrylamide/Bis solution	2.5 mL
Stacking gel buffer	5 mL
10% SDS	0.2 mL
1.5% Ammonium persulfate	1.0 mL
TEMED	15 μ L
Water	11.3 mL

Note: the gel should be de-aerated before addition of ammonium persulfate.

Reducing solution and gel loading buffer for gel electrophoresis:

Sodium dodecyl sulphate	1 g
β -Mercaptoethanol	2 mL
Bromophenol blue	10 mg
Stacking buffer stock	1.5 mL
Sucrose	5 g
Water	6.5 mL

Tris buffered saline-Tween (TBS-T) 20 (pH 7.4):

Tris	1.21 g
NaCl	8.27 g
Tween-20	1 mL
Water	1 L

Transfer buffer:

Tris	3.03 g
Glycine	43.2 g
Methanol	200m L
Water	1 L

Phosphate buffered saline (PBS) (pH 7.4):

NaCl	8g
KCl	0.2 g
Na ₂ HPO ₄	1.81 g
KH ₂ PHO ₄	0.24 g

In 900 mL of milli-Q water, adjust the pH to 7.4 using HCl, and make up the solution to 1 L.

Krebs-HEPES Buffer (pH 7.4):

NaHEPES	5.2 g
NaCl	6.9 g
KCl	0.26 g
CaCl ₂	0.19 g
MgSO ₄	0.14 g
KH ₂ PO ₄	0.21 g
Glucose	1.80 g
0.1% (w/v) bovine serum albumin	
Water	1 Liter

3T3-L1 Lysis buffer (pH 7.4):

Tris/HCl	14.3 g
NaF	2.1 g
Na ₄ O ₇ P ₂ ·10H ₂ O	2.2 g
EDTA	0.29 g
EGTA	0.38 g
Mannitol	45.6 g
Triton X-100	1% (v/v)
Dithiothreitol	0.15 g
Benzamidine	0.16 g

phenylmethane sulfonyl fluoride	0.0174 g
Soybean trypsin inhibitor	5 mg
Water	1 Liter

Coomassie reagent:

Coomassie G-250	100 mg
95% ethanol	50 mL
85% phosphoric acid	100 mL
Distilled water	850 mL

This solution should be stirred, filtered and stored in a dark bottle.

Reagents for amido black staining

Stain:

0.1% (w/v) amido black in 25% (v/v) isopropanol, 10% (v/v) acetic acid,
in water;

Destain solution:

25% (v/v) isopropanol, 10% (v/v) acetic acid in water.

Metformin stock solution for the adipogenesis experiment:

1 M metformin solution:

Metformin (Molecular weight 165.63 g/mole) 1.66 g

3T3-L1 cells growth medium 10 mL

AICAR stock solution for the adipogenesis experiment:

0.1M AICAR solution:

AICAR (Molecular weight 258.2g/mole) 0.258 g

3T3-L1 cells growth medium 10 mL

Metformin stock solution for the HIV-1 inhibition experiment:

1 M metformin solution:

Metformin 1.66 g

PBS 10 mL

AICAR stock solution for the HIV-1 inhibition experiment:

0.1 M AICAR: 0.258 g

PBS 10 mL

IBMX solution:

IBMX	50 mg
Warm methanol	1 mL

Dexamethasone solution:

Dexamethasone	10 mg
Ethanol	10 mL
PBS	190 mL

Note: the PBS was filtered with a Whatman paper before use.

APPENDIX III

RAW DATA

Table 1: Absorbance readings of Oil red O on day 0 and day 8 of 3T3-L1 tissue culture.

	Day 0	Day 8
Experiment 1	0.0250	0.1161
Experiment 2	0.0303	0.0942
Experiment 3	0.0300	0.1004
Experiment 4	0.0230	0.0846
Experiment 5	0.0444	0.0635
Experiment 6	0.0247	0.0574
Mean	0.0296	0.0860
Standard deviation	0.0079	0.0224

Table 2: Absorbance readings of Oil red O for different concentrations of Metformin on day 8.

	0 mM	2 mM	4 mM	8 mM	16 mM
Experiment 1	0.1161	.1509	.0936	.0648	.0604
Experiment 2	0.0942	.1005	.0794	.0635	.0651
Experiment 3	0.1004	.1035	.0768	.0520	.0555
Experiment 4	0.0846	.0768	.0405	.0400	.0271
Experiment 5	0.0635	.0520	.0368	.0377	.0365
Experiment 6	0.0574	.0555	.0161	.0333	.0385
Mean	0.0860	.0899	.0572	.0486	.0472
Standard deviation	0.0224	.0369	.0303	.0136	.0152

Table 3: Absorbance readings of Oil red O of 0 mM and 1 mM of AICAR on day 8.

	0 mM	1 mM
Experiment 1	.1161	.0757
Experiment 2	.0942	.0690
Experiment 3	.1004	.0701
Experiment 4	.0846	.0475
Experiment 5	.0635	.0512
Experiment 6	.0574	.0473
Mean	.0860	.0601
Standard deviation	.0224	0128

Table 4: Kodak ID Image Analysis v3.6 net intensity values of phospho-AMPK on day 8 of adipogenesis. For AICAR 1 mM, metformin 16 mM, and the negative control.

	AICAR	Metformin	Negative control
Experiment 1	16785.030	33116.450	8291.230
Experiment 2	56277.480	31080.280	11880.640
Experiment 3	15245.830	81197.310	11473.500
Experiment 4	90933.280	28749.790	4731.070
Experiment 5	200949.650	303491.000	52333.740
Mean	76038.254	95526.966	17742.036
Standard deviation	76521.027	118281.463	19550.188

Table 5: P24 values for NaCl treated cells and untreated cells on day 2 of tissue culture.

	NaCl treated cells	Untreated cells
Experiment 1	16.8000	2.2250
Experiment 2	2.1760	0.950
Experiment 3	0.6820	0.1310
Experiment 4	0.7120	0.2630
Experiment 5	1.5320	0.4180
Experiment 6	1.0090	0.2630
Experiment 7	1.4470	0.3360
Mean	3.480	5.897
Standard deviation	0.655	0.741

Table 6: P24 values in ng/mL for the control culture and 4, 8, and 16 mM metformin treated cultures, after 2 days of tissue culture.

	Control cells	Metformin 4 mM	Metformin 8 mM	Metformin 16 mM
Experiment 1	5.569	2.219	1.456	1.484
Experiment 2	55.989	26.637	20.980	13.206
Experiment 3	1.725	0.442	0.405	0.394
Experiment 4	1.156	0.634	0.378	0.461
Experiment 5	4.799	2.811	1.735	2.097
Experiment 6	1.447	0.226	0.163	0.173
Experiment 7	2.176	0.351	0.462	0.625
Experiment 8	0.682	0.174	0.209	0.204
Mean	9.193	4.187	3.224	2.330
Standard deviation	18.990	9.126	7.199	4.446

Table 7: P24 values, in table 6, expressed as percentage of the control.

	Control cells	Metformin 4 mM	Metformin 8 mM	Metformin 16 mM
Experiment 1	100.00	39.84	26.14	26.64
Experiment 2	100.00	47.57	37.47	23.59
Experiment 3	100.00	25.62	23.48	22.84
Experiment 4	100.00	54.84	32.70	39.89
Experiment 5	100.00	58.57	36.15	43.70
Experiment 6	100.00	15.62	11.26	12.00
Experiment 7	100.00	16.13	21.23	28.72
Experiment 8	100.00	25.51	30.64	29.91
Mean	100.00	35.462	27.384	28.411
Standard deviation	0.00	17.065	8.718	9.961

Table 8: P24 values in ng/mL for the control U1 culture, 0.2 mM, 0.35 mM, and 0.4 mM AICAR treated U1 cells.

	Control cells	AICAR 0.2 mM	AICAR 0.35 mM	AICAR 0.4 mM
Experiment 1	1.156	0.618	0.113	0.101
Experiment 2	5.569	6.058	1.539	1.449
Experiment 3	16.376	7.805	1.482	0.266
Experiment 4	55.939	10.566	2.721	1.965
Experiment 5	4.797	2.413	1.337	1.422
Experiment 6	1.725	0.555	0.262	0.255
Experiment 7	0.682	0.755	0.157	0.162
Experiment 8	2.176	1.884	0.307	0.128
Experiment 9	1.447	0.673	0.268	0.168
Mean	9.985	3.481	0.910	0.657
Standard deviation	17.908	3.730	0.907	0.734

Table 9: P24 values, in table 8, expressed as percentage of the control.

	Control cells	AICAR 0.2 mM	AICAR 0.35 mM	AICAR 0.40 mM
Experiment 1	100.0	53.5	9.8	8.7
Experiment 2	100.0	108.7	27.6	27.6
Experiment 3	100.0	47.7	9.0	1.6
Experiment 4	100.0	18.9	4.9	3.5
Experiment 5	100.0	50.3	27.9	29.6
Experiment 6	100.0	32.2	15.2	14.8
Experiment 7	100.0	111.0	23.0	23.8
Experiment 8	100.0	86.6	14.1	5.9
Experiment 9	100.0	46.5	18.5	11.6
Mean	100.0	61.7	16.7	14.131
Standard deviation	0.0	32.8	8.2	10.5

Table 10: Kodak 1D Image Analysis Software v3.6 net intensity values for nuclear NF- κ B in U1 cells.

	Untreated cells	Metformin 16 mM	AICAR 0.40 mM
Experiment 1	575358.290	256588.460	106952.000
Experiment 2	120091.680	15080.930	22492.000
Experiment 3	10843.640	8612.590	9744.980
Experiment 4	41714.930	13671.830	9897.220
Experiment 5	81529.000	40703.000	18228.50
Mean	165907.508	140736.498	33462.940
Standard deviation	232560.404	166947.786	41445.677

Table 11: Kodak 1D Image Analysis Software v3.6 net intensity values for cytoplasmic NF- κ B in U1 cells.

	Untreated cells	Metformin 16 mM	AICAR 0.40 mM
Experiment 1	6323.490	2579.370	14703.930
Experiment 2	150924.640	163644.820	237380.230
Experiment 3	155612.000	217561.480	332234.920
Mean	104286.710	127928.557	194773.027
Standard deviation	84871.003	111852.874	162996.972

Table 12: concentration ($\mu\text{g}/\text{mL}$) of protein extracts from U1 cells cytoplasm.

	Negative control	Metformin 16 mM	AICAR 1 mM
Experiment 1	2083.0	1362.4	1449.4
Experiment 2	1958.3	1696.0	1638.6
Experiment 3	1782.0	1588.8	1840.41
Experiment 4	641.6	680.3	523.1
Experiment 5	607.1	527.0	626.1
Mean	1414.4	1170.9	1215.5
Standard deviation	729.2	534.4	602.3

Table 13: concentration ($\mu\text{g}/\text{mL}$) of protein extracts from U1 cells nucleus.

	Negative control	Metformin 16 mM	AICAR 1 mM
Experiment 1	1506.6	1184.3	2337.8
Experiment 2	1177.5	1067.7	687.9
Experiment 3	2399.2	1054.6	1200.8
Experiment 4	544.1	477.6	570.6
Experiment 5	293.4	481.9	603.4
Mean	1184.1	853.2	1080.1
Standard deviation	834.2	344.7	747.8

LIST OF REFERENCES

1. Kemp, B.E., D. Stapleton, D. J. Campbell, et al., *AMP-activated protein kinase, super metabolic regulator*. Biochemical Society Transactions, 2003. **31**: p. 162-168.
2. Hardie, D.G., *The AMP-activated protein kinase pathway-new players upstream and downstream*. Journal of Cell Science, 2004. **117**: p. 5479-5487.
3. Leclerc, I. and G.A. Rutter, *AMP-Activated protein kinase: A new β -cell glucose sensor?* . Diabetes, 2004. **53**: p. S67-S74.
4. Rossmeis, I.M., P. Flachs, P. Brauner, et al., *Role of energy charge and AMP-activated protein kinase in adipocytes in the control of body fat stores*. International Journal of Obesity, 2004. **28**: p. S38-S44.
5. Shaw, R.B., M. Kosmatka, N. Bardeesy, et al., *The tumor suppressor LKB1 kinase directly activates AMP-activated kinase and regulates apoptosis in response to energy stress*. Proceedings of the National Academy of Sciences USA, 2004. **101**: p. 3329-3335.
6. Leff, T., *AMP-activated protein kinase regulates gene expression by direct phosphorylation of nuclear proteins* Biochemical Society Transactions, 2001. **31**: p. 224-227.
7. Asin, S., G. D. Bren, E. M. Carmona, et al., *NF- κ B cis-acting motifs of the human immunodeficiency virus (HIV) long terminal repeat*

- regulate HIV transcription in human macrophages*. Journal of virology, 2001. **75**: p. 11408 -11416.
8. Winder, W.W. and D.G. Hardie, *AMP-activated protein kinase, a metabolic master switch: possible roles in Type 2 diabetes*. American Journal of Physiology: Endocrinology and Metabolism, 1999. **277**: p. E1-10.
 9. Zhou, G.M., R. Myers, Y. Li, et al., *Role of AMP-activated protein kinase in mechanism of metformin action*. Journal of Clinical Investigation, 2001. **108**: p. 1167-1174.
 10. Adams, J., Z-P. Chen, B. J. W. van Denderen, et al., *Intrasteric control of AMPK via the γ_1 subunit AMP allosteric regulatory site*. Protein Science, 2004. **13**: p. 155-165.
 11. Winder, W.W., D.G. Hardie, K. J. Mustard, et al., *Long-term regulation of AMP-activated protein Kinase and acetyl-CoA carboxylase in skeletal muscle*. Biochemical Society Transactions, 2003. **31**: p. 182-185.
 12. Durante, P.E., K. J. Mustard, S. H. Park, et al., *Effects of endurance training on activity and expression of AMP-activated protein kinase isoform in rat muscles*. American Journal of Physiology: Endocrinology and Metabolism, 2002. **283**: p. E178-E186.
 13. Neumann, D., U. Schlattner and T. Wallimann, *A molecular approach to the concerted action of kinases involved in energy*

- homeostasis*. Biochemical Society Transactions, 2003. **31**: p. 169-174.
14. Nielsen, J.N., S. B. Jørgensen, B.V. C. Frøsig, et al., *A possible role for AMP-activated protein kinase in exercise-induced glucose utilization: insights from humans and transgenic animals*. Biochemical Society Transactions, 2003. **31**: p. 186-190.
 15. <http://www.3dchem.com/molecules.asp?ID=182>, Metformin@3Dchem.com Glucophage, 2006.
 16. Kirpichnikov, D., S. I. McFarlane and J.R. Sowers., *Metformin: An update*. Annals of Internal Medicine, 2002. **137**: p. E25-E33.
 17. Cleasby, M.E., N. Dzamko, B. D. Hegarty, et al., *Metformin prevents the development of acute lipid-induced insulin resistance in the rat through altered hepatic signaling mechanism*. Diabetes, 2004. **53**: p. 3258-3266.
 18. Musi, N., M. F. Hirshman, J. Nygren, et al., *Metformin increases AMPK-activated Protein Kinase Activity in Skeletal Muscle of Subjects with Type 2 Diabetes*. Diabetes, 2002. **51**: p. 2074-2081.
 19. Witters, L.A., *The blooming of the French lilac*. Journal of Clinical Investigation, 2001. **108**: p. 1105-1107.
 20. Josie, M.M.E., L. A. Donnelly, A. M. Emslie-Smith, et al., *Metformin and reduced risk of cancer in diabetic patients*. British Medical Journal, 2005. **330**: p. 1304-1305.

21. Hawley, S.A., A. E. Gadall, G. S. Olsen, et al., *The Antidiabetic Drug Metformin Activates the AMP-Activated Protein Kinase Cascade via an Adenine Nucleotide-Independent Mechanism*. *Diabetes*, 2002. **51**: p. 2420-2425.
22. AL-Jebawi, A.F., M. N. Lassman and N.N. Abourizk, *Lactic acidosis with therapeutic metformin blood level in a low-risk diabetes patient*. *Diabetes Care*, 1998. **21**: p. 1364-1365.
23. Tiikkainen, M., A-M. Hakkinen, E. Korshennikova, et al., *Effects of rosiglitazone and metformin on liver fat content, hepatic insulin resistance, insulin clearance, and gene expression in adipose tissue in patients with patients with type 2 diabetes*. *Diabetes*, 2004. **53**: p. 2169-2176.
24. Ruderman, N.B., A. K. Saha and E.W. Kraegen, *Minireview: Malonyl CoA, AMP-Activated Protein Kinase, and Adiposity*. *Endocrinology*, 2003. **144**: p. 5166-5171.
25. Habinowski, S.A. and L.A. Witters, *The Effects of AICAR on Adipocyte Differentiation of 3T3-L1 Cells*. *Biochemical Biophysical Research Communications*, 2001. **286**: p. 852-856.
26. Lochhead, P.A., I. P. Salt, k. S. Walker, et al., *5-Aminoimidazole-4-carboxamide riboside mimics the effects of insulin on the expression of the 2 key gluconeogenic genes PEPCCK and glucose-6-phosphatase*. *Diabetes*, 2000. **49**: p. 896-903.

27. Ferré, P., D. Azzout-Marniche and F. Foufelle., *AMP-activated protein kinase and hepatic genes involved in glucose metabolism*. Biochemical Society Transactions, 2003. **31**: p. 220-223.
28. Vinod, N.K., S. M. Rupinder, C. Murugesan, et al., *Myocardial ischaemic pre-conditioning*. Indian Journal of Anaesthesia, 2004. **48**: p. 93-99.
29. Fabian, T.C., M. J. Fabian, J. M. Yockey, et al., *Acadesine and lipopolysaccharide-evoked pulmonary dysfunction after resuscitation from traumatic shock*. Surgery, 1996. **119**: p. 302-315.
30. Hong, S.-P., F. C. Lieper, A. Woods, et al., *Activation of yeast Snf1 and mammalian AMP-activated protein kinase by upstream kinases*. Proceedings of the National Academy of Sciences USA, 2003. **100**: p. 8839-8843.
31. Hawley, S.A., J. Boudeau, J. L. Reid, et al., *Complexes between the LKB1 tumor suppressor, STRAD α/β and MO25 α/β are upstream kinases in the AMP-activated protein kinase cascade*. Journal of Biology, 2003. **2**: p. 28.1-28.16.
32. Suzuki, A., G-I. Kusakai, A. Kishimoto, et al., *IGF-1 phosphorylates AMPK- α subunit in ATM-dependent and LKB1-independent manner*. Biochemical and Biophysical Research Communications, 2004. **324**: p. 986-992.

33. Lizcano, J.M., O. Goransson, R. Toth, et al., *LKB1 is a master kinase that activates 13 kinases of the AMPK subfamily, including MARK/PAR-1*. The European Molecular Biology Organization Journal, 2004. **23**: p. 833-843.
34. Hurley, R.L., K. A. Anderson, J. M. Franzone, et al., *The Ca^{++} /calmodulin-dependent protein kinase kinases are AMP-activated protein kinase kinases*. Journal of Biological Chemistry, 2005. **280**: p. 29060-29066.
35. Fryer, L.G.D., E. Hajduch, F. Rencurel, et al., *Activation of glucose transport by AMP-activated protein kinase via stimulation of nitric oxide synthase*. Diabetes, 2000. **49**: p. 1978-1985.
36. Chen, Z.-P., G. K. McConell, B. J. Michell, et al., *AMPK signaling in contracting human skeletal muscle: acetyl-CoA carboxylase and nitric oxide synthase phosphorylation* American Journal of Physiology: Endocrinology and Metabolism, 2000. **279**: p. E1202-E1206.
37. Violett, B., F. Andreoli, S. B. Jorgensen, et al., *Physiological role of AMP-activated protein kinase (AMPK) insights from knockout mouse models*. Biochemical Society Transactions, 2003. **31**: p. 216-219.
38. Zang, M., A. Zuccollo, X. Hou, et al., *AMP-activated Protein Kinase Is Required for the Lipid-lowering Effect of Metformin in Insulin-*

- resistant Human HepG2 Cells*. Journal of Biological Chemistry, 2004. **279**: p. 47898-47905.
39. Villena, J.A., B. Viollet, F. Andreelli, et al., *Induced adiposity and adipocyte hypertrophy in mice lacking the AMP-activated protein kinase- α_2 subunit*. Diabetes, 2004. **53**: p. 2242-2249.
 40. Yin, W., J. Mu and M.J. Birnbaum, *Role of AMP-activated Protein Kinase in Cyclic AMP-dependent Lipolysis In 3T3-L1 Adipocytes*. Journal of Biological Chemistry, 2003. **278**: p. 43074-43080.
 41. Zimmet, P., K. G. M. M. Alberti, J. Shaw, et al., *Global and societal implications of the diabetes epidemic*. Nature, 2001. **414**: p. 782-787.
 42. Turnpenny, P. and S. Ellard, *Emery's Elements of Medical Genetics*. 12th ed, ed. A. Stibbe. 2005: Elsevier Churchill Livingstone.
 43. Baynes, J.W. and D.H. Marek, *Medical Biochemistry*, ed. A. Stibbe. 2005, Amsterdam: Elsevier Mosby.
 44. Weir, G.C. and S.B. Weir, *Islets of Langerhans: The puzzle of intraislet interactions and their relevance to diabetes*. Journal of Clinical Investigation, 1990. **85**: p. 983-987.
 45. Camp, H.S., D. Ren and T. Leff, *Adipogenesis and fat cell-function in obesity and diabetes*. Trends in Molecular Medicine, 2002. **8**: p. 442-446.

46. Minokoshi, Y. and B.B. Khan, *Role of AMP-activated protein kinase in leptin-induced fatty acid oxidation in muscle*. Biochemical Society Transactions, 2003. **31**: p. 196-201.
47. Bauman, C.A. and A.R. Saltiel, *Spatial compartmentalization of signal transduction in insulin action*. BioEssays, 2001. **23.2**: p. 215-222.
48. Punyadeera, C., M.T.v.d. Merwe', N. J. Crowther , et al., *Weight-related differences in glucose metabolism and free fatty acid production in two South African population groups*. International Journal of Obesity, 2001. **25**: p. 1196-1205.
49. Tsukinoki, R., K. Morimoto and K. Nakayama, *Association between lifestyle factors and plasma adiponectin levels in Japanese men*. Lipid in Health and Disease, 2005. **4**: p. 27.
50. Wellen, K.E. and G.S. Hotamisligil, *Inflammation, stress, and diabetes*. The Journal of Clinical Investigation, 2005. **115**: p. 1111-1119.
51. Hida, K., J. Wada, J. Eguchi, et al., *Visceral adipose tissue-derived serine protease inhibitor: A unique insulin-sensitizing adipocytokine in obesity*. Proceedings of the National Academy of Sciences USA, 2005. **102**: p. 10610-10615.
52. Ruderman, N.B., J. M. Cacicedo, S. Itani, et al., *Malonyl-CoA and AMP-activated protein kinase (AMPK): Possible links between*

- insulin resistance in muscle and early endothelial cell damage in diabetes*. Biochemical Society Transactions, 2003. **31**: p. 202-206.
53. Steinberg, G.R., A. C. Smith, B. J. W. van Denderen, et al., *AMP-activated protein kinase is not down-regulated in human skeletal muscle of obese females*. The Journal of Clinical Endocrinology and Metabolism, 2005. **89**: p. 4575-4580.
54. Musi, N., N. Fujii N, M. F. Hirschman, et al., *AMPK activated protein kinase AMPK is activated in muscle of subjects with type 2 diabetics during exercise*. Diabetes, 2001. **50**: p. 921-927.
55. Hojlund, K., K. J. Mustard, P. Staehr, et al., *AMPK activity and isoform protein expression are similar in muscle of obese subjects with and without type 2 diabetes*. American Journal of Physiology: Endocrinology and Metabolism, 2004. **286**: p. E239-244.
56. Miller, R.J., J. S. Cairns, S. Bridges, et al., *Human Immunodeficiency Virus and AIDS: Insight from Animal Lentiviruses*. Journal of virology, 2000. **74**: p. 7187-7195.
57. Sharp, P.M., G. M. Shaw and B.H. Hahn, *Simian immunodeficiency virus infection of chimpanzees* Journal of Virology, 2005. **79**: p. 3891-3902.
58. Mims, C., H. M. Dockrell, R. V. Goering, et al., *Medical Microbiology*. 3 ed. 2004, International: Elsevier Mosby.
59. Kinchington, D. and N. Fitch, *Discovery and classification of HIV/Human Immunodeficiency Virus*, in *Human Immunodeficiency*

- Virus*, D.D. Richman, Editor. 2003, International Medical press:
London.
60. <http://www.iavi.org>, International AIDS Vaccine Initiative, 2006.
61. <http://www.washington.edu/.../columns/dec00/cells.4.htm>,
University of Washington, 2004.
62. http://www.scap4.org/album23a_007.htm, Stanislaus Community
Assistant Project, 2004.
63. Cheng, H., J. Tarnok and W.P. Parks, *Human immunodeficiency
virus type 1 genome activation induced by human T-cell leukemia
virus type 1 Tax protein is through cooperation of NF- κ B and Tat.*
Journal of virology, 1998. **72**: p. 6911 - 6916.
64. Horuk, R., *Chemokine receptors and HIV type 1: the fusion of two
major research fields.* *Immunology Today*, 1999. **20**: p. 89 - 94.
65. <http://www.aids-info.ch/e-te/aaas-e-imm.htm>, AIDS Information
Switzerland, 2006.
66. Cullen, B.R. and W.R. Greene, *Functions of the auxiliary gene
products of the human immunodeficiency virus type 1*
Virology, 1990. **178**: p. 1-5.
67. Malim, M.H., J. Hauber, S-Y. Le, et al., *The HIV-1 rev trans-
activator acts through a structured target sequence to activate
nuclear export of unspliced viral mRNA.*
Nature, 1989. **338**: p. 254-257.

68. Laspia, M.F., A. P. Rice and M.B. Mathews, *HIV-1 Tat protein increases transcriptional initiation and stabilizes elongation*. *Cell*, 1989. **59**: p. 283-292.
69. Vermeulen, L., G. De Wilde, P. van Damme, et al., *Transcriptional activation of the NF- κ B activation p65 subunit by mitogen- and stress-activated protein kinase-1 (MSK-1)*. *The European Molecular Biology Organization Journal*, 2003. **22**: p. 1313-1324.
70. Duran, A., M. T. Diaz-Meco and J. Moscat, *Essential role of relA ser311 phosphorylation by ζ PKC in NF- κ B transcriptional activation*. *The European Molecular Biology Organization Journal*, 2003. **22**: p. 3910-3918.
71. Chene, L., M. T. Nugeyre, F. Barre-Sinoussi, et al., *High-level replication of human immunodeficiency virus in thymocytes requires NF- κ B activation through interaction with thymic epithelial cells*. *Journal of Virology*, 1999. **73**: p. 2064-2073.
72. Hiscott, J., H. Know and P. Genin, *Hostile takeover: viral appropriation of NF- κ B*. *The Journal of Clinical Investigation*, 2001. **107**: p. 143-151.
73. Duh, E.J., W. J. Maury, T. M. Folks, et al., *Tumor necrosis factor α activates human immunodeficiency virus type 1 through induction of nuclear factor binding to the NF- κ B sites in the long terminal repeat*. *Proceedings of the National Academy of Sciences USA*, 1989. **86**: p. 5974 - 5978.

74. Paya, C.V., R. M. Ten, C. Bessia, et al., *NF- κ B-dependent induction of the NF- κ B p50 subunit gene promoter underlies self-perpetuation of human immunodeficiency virus transcription in monocytic cells.* . Proceedings of the National Academy of Sciences USA, 1992. **89**: p. 7826-7830.
75. Wu, X., H. Motoshima, K. Mahadev, et al., *Involvement of AMP-activated protein kinase in glucose uptake stimulated by globular domain of adiponectin in primary rat adipocytes.* Diabetes, 2003. **52**: p. 1355-1363.
76. Marzio, G., M. Tyagy, M. I. Gutierrez, et al., *HIV-1 tat transactivation recruits p300 and CREB-binding protein histone acetyltransferases to the viral promoter.* Proceedings of the National Academy of Sciences USA, 1998. **95**: p. 13519-13524.
77. Fitch, N., *Antiretroviral therapy 1: principles and current practice*, in *Human immunodeficiency virus*, D. Richman, Editor. 2003, London: International medical press.
78. Janke, J.S., K. Gorzelniak, F. C. Luft, et al., *Mature adipocytes inhibit in vitro differentiation of human preadipocytes via angiotensin type 1 receptors.* Diabetes, 2002. **51**: p. 1699-1707.
79. Bradford, M.M., *A rapid and sensitive method for the quantification of microgram quantities protein.* Analytical Biochemistry, 1976. **72**: p. 248-254.

80. Shapiro, L., G. B. Pott and A.M. Ralston, *Alpha-1-antitrypsin inhibits human immunodeficiency virus type 1*. The Federation of American Societies for Experimental Biology Journal, 2001. **15**: p. 115-122.
81. Skolnik, P.R., M. F. Rabbi, J-M. Mathys, et al., *Stimulation of Peroxisome Proliferator-Activated Receptors α and γ Blocks HIV-1 Replication and TNF α Production in Acutely Infected Primary Blood Cells, Chronically Infected U1 Cells, and Alveolar Macrophages From HIV-Infected Subjects*. Journal of Acquired Immune Deficiency Syndromes, 2002. **31**: p. 1-10.
82. Griffin, S., *Viral replication*, in *Human immunodeficiency virus*, D.D. Richman, Editor. 2003, International Medical Press. p. 3.1-3.16.
83. Winder, W.W., H. A. Wilson and D.G. Hardie, *Phosphorylation of rat muscle acetyl-CoA carboxylase by AMP-activated protein kinase and protein kinase A*. Journal of Applied Physiology, 1997. **82**: p. 219-225.
84. Dyck, J.R., N. Kudo, A. J. Barr, et al., *Phosphorylation control of cardiac acetyl-CoA carboxylase by cAMP-dependent protein kinase kinase and 5'-AMP activated protein kinase*. European Journal of Biochemistry, 1999. **262**: p. 184-190.
85. Guigas B., L. Bertrand, N. Taleux, et al., *5-Aminoimidazole-4-Carboxamide-1- β -D-Ribofuranoside and metformin Inhibit Hepatic*

Glucose Phosphorylation by an AMP-Activated protein Kinase-Independent Effect on Glucokinase Translocation. Diabetes, 2006. 55: p. 865-874.

86. Hannibal, M.C., D. M. Markovitz, N. Clark, et al., *Differential activation of human immunodeficiency virus type1 and type 2 transcription by specific T-cell activation signals.* Journal of virology, 1993. 67: p. 5035-5040.
87. Hadigan, C., J. Rabe and S. Grinspoon, *Sustained Benefits of Metformin Therapy on Markers of Cardiovascular Risk in Human Immunodeficiency Virus-Infected Patients with Fat Redistribution and Insulin Resistance.* The Journal of Endocrinology & Metabolism, 2006. 87: p. 4611-4615.